A natural single nucleotide mutation in the small regulatory RNA ArcZ of *Dickeya solani* switches off the antimicrobial activities against yeast and bacteria.

Running title: ArcZ role in *Dickeya solani* anti-microbial activities

Authors: Brual T[1$], Effantin G[1$], Baltenneck J[1], Attaiech L[2], Grosbois C[1], Royer M[4], Cigna J[5], Faure D[6], Hugouvieux-Cotte-Pattat N[1] & Gueguen E[1]*.

Affiliation:

[1] Univ Lyon, Université Claude Bernard Lyon1, CNRS, INSA Lyon, UMR5240 MAP, F-69622, LYON, France

[2] CIRI, Centre International de Recherche en Infectiologie, Team "Horizontal gene transfer in bacterial pathogens" (Horigene), Inserm, U1111, Université Claude Bernard Lyon 1, CNRS, UMR5308, Ecole Normale Supérieure de Lyon, Univ Lyon, 69100, Villeurbanne, France.

[4] CIRAD, UMR PHIM, Montpellier, F-34398, France

[5] French Federation of Seed Potato Growers (FN3PT-inov3PT), 43-45 rue de Naples, 75008 Paris, France

[6] Paris-Saclay University, CNRS, CEA, Institute for Integrative Biology of the Cell (I2BC), Gif-sur-Yvette, France

[$] These authors contributed equally to this work.

*corresponding author: erwan.gueguen@univ-lyon1.fr

Orcid I.D.

G.E. 0000-0001-8784-1491

H-C-P.N 0000-0002-4322-160X

F. D. 0000-0002-5379-8867

28 R. M. 0000-0003-0421-982X

29 A. L. 0000-0002-6188-1839

30 E.G. 0000-0002-7296-0831

31 B.J. 0000-0001-8456-4126

32 C. J. 0000-0002-1219-7096

33 B.T 0000-0001-5179-8882

34

35

36

37 Key words: *Dickeya solani*, secondary metabolites, oocydin, zeamine, solanimycin, bacteria,

38 yeast, fungi, streptomyces, candida, sRNA, arcZ, SNP.

39

ABSTRACT

The necrotrophic plant pathogenic bacterium *Dickeya solani* emerged in the potato agrosystem in Europe. All isolated strains of *D. solani* contain several large polyketide synthase/non-ribosomal peptide synthetase gene clusters. Analogy with genes described in other bacteria suggests that the clusters *ooc* and *zms* are involved in the production of secondary metabolites of the oocydin and zeamine families, respectively. A third cluster that we named *ssm* for *solani* secondary metabolite had an unknown function. In this study, we constructed mutants impaired in each of the three secondary metabolite clusters *ssm*, *ooc*, and *zms* to compare first the phenotype of the *D. solani* wild-type strain D s0432-1 with its associated mutants. We demonstrated the antimicrobial functions of these three PKS/NRPS clusters against bacteria, yeasts or fungi. The secondary metabolite cluster *ssm*, conserved in several other *Dickeya* species, produces a secondary metabolite inhibiting yeasts. Phenotyping and comparative genomics of different *D. solani* wild-type isolates revealed that the small regulatory RNA ArcZ plays a major role in the control of the clusters *ssm* and *zms*. A single-point mutation, conserved in some *Dickeya* wild-type strains, including the type strain IPO 2222, impairs the ArcZ function by affecting its processing into an active form.

197 words

AUTHOR SUMMARY

The development of new antibacterial molecules is critical in tackling the emergence of new pathogens or bacterial strains resistant to already available antibiotics. Bacterial phytopathogens can potentially synthesize novel compounds capable of targeting a specific type of microorganism. *Dickeya solani* is the only of the twelve described *Dickeya* species that has the three secondary metabolic pathways *ssm*, *ooc* and *zms*. An investigation of the functions of these three clusters allowed us to identify the anti-yeast activity of the *ssm* cluster,

a potential new molecule of clinical importance. By comparing the antimicrobial activity of several *Dickeya solani* strains, we identified the small RNA regulator ArcZ as a critical regulator in the activation of the *ssm* and *zms* clusters. Our study showed that single-nucleotide polymorphisms of sRNA encoding genes can have huge impacts on bacterial phenotypes. It is thus critical to pay attention to the allele diversity of sRNA genes.

148 words

77 **INTRODUCTION**

78

79 Bacterial phytopathogens of the genus *Dickeya* and *Pectobacterium* are pectinolytic
80 necrotrophic bacteria with a broad host plant spectrum [1,2]. These members of the family
81 *Pectobacteriaceae* [3] cause substantial agricultural losses worldwide by affecting many
82 vegetables, ornamentals and crops, of which the potato is the most important economically.
83 These bacteria are able to invade and degrade the plant tissues through the coordinated
84 expression of genes encoding virulence factors, with a major role of pectate lyases that
85 dissociate the plant cell wall constituents [4].
86 The *Dickeya* genus was established in 2005 [5], resulting from the reclassification of
87 *Pectobacterium chrysanthemi* (formerly *Erwinia chrysanthemi*). To date, twelve species of
88 *Dickeya* have been described, *D. aquatica*, *D. chrysanthemi*, *D. dadantii, D. dianthicola* , *D.*
89 *fangzhongdai*, *D. lacustris*, *D. oryzae*, *D. parazeae, D. poaceiphila*, *D. solani*, *D. undicola*, and
90 *D. zeae* [5–14].
91 The species *D. solani* was officially established in 2014 [9] but *D. solani* isolates have attracted
92 attention since its emergence on the potato agrosystem in Europe in the early 2000s. It causes
93 symptoms in both subtropical and temperate climates. Many scientific efforts have been made
94 to provide information on this phytopathogen, resulting in 76 *D. solani* genomes available in
95 May 2021 [15]. Comparative genomics was performed to identify the genetic basis for the
96 different levels of virulence between *D. solani* strains [15–20]. Most *D. solani* strains isolated
97 from different regions show a low level of genetic variation, suggesting a clonal origin [20].
98 The *D. solani* genomes share a high similarity and synteny with those of the model strain *D.*
99 *dadantii* 3937, prompting comparison between the two species. Only a few hundred genes
100 were specific to each species, including a few dozen distinctive genomic regions [16,17].
101 Three of these regions encode polyketide synthases (PKS), non-ribosomal peptide
102 synthetases (NRPS) and amino acid adenylation domain proteins, which are typically involved
103 in the production of secondary metabolites [16].

104 PKSs and NRPSs are able to synthesize molecules by sequential condensation of carboxylic
105 acids and amino acids, respectively. PKS and NRPS modules can combine together to form
106 hybrid PKS/NRPS systems capable of producing compounds of great structural diversity [21].
107 The molecules synthesized may have siderophore, antibiotic or phytotoxic properties that
108 promote the virulence of a plant pathogen. Three PKS/NRPS clusters are present in all
109 sequenced *D. solani* strains and found in a few other *Dickeya* species and related genera:
110 *ooc*, *zms*, and a cluster of unknown function [22]. In *Serratia plymuthica,* the cluster *ooc* is
111 involved in the synthesis of oocydin A, a halogenated macrolide with antifungal and anti-
112 oomycete activity [23]. The cluster *zms*, previously found in the genomes of *S. plymuthica* and
113 *Dickeya oryzae,* leads to the biosynthesis of a polyamino-amide antibiotic, zeamine [24,25].
114 The third cluster *ssm* (for *solani* secondary metabolite) is found in a few *Dickeya* species but
115 the nature and function of the synthesized molecule are unknown. To elucidate the
116 contribution of the *ssm*, *ooc* and *zms* clusters of *D. solani* in competition with other living
117 organisms, we constructed mutants of each of the three loci involved in the biosynthesis of
118 secondary metabolites in the highly virulent *D. solani* strain D s0432-1. We showed that the
119 *D. solani* D s0432-1 clusters *zms* and *ooc,* encoding zeamine and oocydin biosynthesis, are
120 involved in growth inhibition of bacteria and fungi, respectively. Recently we, and others
121 identified the third cluster as implicated in *Dickeya solani*'s ability to inhibit the growth of
122 different yeast species [26,27]. We named this cluster *ssm* (for *solani* secondary metabolite)
123 while Matilla and colleagues named it sol (for solanimycin, the molecule produced by this
124 cluster). Finally, the comparative analysis of the genomes and phenotypes of several wild-
125 type *D. solani* strains revealed the fundamental role of the small RNA ArcZ. This sRNA plays
126 a major role in the regulation of the *ssm* and *zms* clusters, which can be disrupted by a
127 mutation in the *arcZ* sequence, conserved in some natural isolates.

128

129

130

131 **RESULTS**

132

133 **Description and distribution of the three selected PKS/NRPS secondary metabolite**

134 **clusters of *D. solani*.**

135

136 The gene clusters encoding complex NRPS and PKS involved in the production of secondary

137 metabolites were named *ssm*, *ooc* and *zms,* respectively (Fig. 1A). Their distribution in

138 *Dickeya* species is summarized in figure 1B (see also Table S1 for a complete list of the

139 *Dickeya* strains with the indication of the presence or absence of each cluster).

140 The ~42-kbp cluster *ssm* contains the 12 genes *ssmABCDEFGHIJKL* (Fig. 1A). It is widely

141 conserved in the genus *Dickeya*, *i.e.*, in all sequenced *D. solani, D. aquatica, D. fangzhongdai,*

142 *D. poaceiphila* and *D. zeae* genomes, in some *D. dadantii* strains (such as NCPPB 898,

143 NCPPB 3537, DSM18020, but not the model strain 3937), in some *D. undicola* strains (FVG1,

144 FVG10), and in some *D. oryzae* strains (such as S20 and FVG03). The structure of the

145 metabolite produced from this cluster has not been elucidated yet but the function of this

146 cluster has been described by us in a 2021 preprint article [27] and others in 2022 [26]. The

147 *ssm* cluster produces solanimycin that targets yeast.

148 The ~80-kbp cluster *ooc* (Fig. 1A) is highly similar to the *oocBCDEFGJKLMNOPQRSTUVW*

149 cluster of *S. plymuthica* A153. It is present in all the sequenced genomes of *D. solani* and *D.*

150 *dianthicola*, in some *D. oryzae* strains (such as ZYY5, EC1, DZ2Q and ZJU1202) and in a few

151 other species. In *S. plymuthica* A153, disruption of this gene cluster abolished bioactivity

152 against the fungi *Verticillium dahliae* and the oomycetes *Pythium ultimum*. This cluster

153 produces oocydin A [23], a chlorinated macrolide, powerfully active against plant pathogenic

154 oomycetes [28]. Since various *D. solani* strains inhibit *V. dahliae* and *P. ultimum* growth [29],

155 it was suggested, on the basis of gene sequence homologies and similar cluster organization,

156 that *D. solani* also produces oocydin A.

157 The ~55-kbp cluster *zms* encodes mixed fatty acid synthase FAS/PKS and hybrid NRPS/PKS

158 enzymes (Fig.1A). Its genomic organization is identical to the *D. oryzae* EC1 zeamine cluster

159 and related to the *S. plymuthica* AS12 zeamine cluster [24,30]. While the
160 *zmsABCDEFGIJKLMNPQRS* cluster directing zeamine biosynthesis is present only in a few
161 *D. oryzae* strains, it is conserved in all the sequenced *D. solani* and *D. fangzhongdai* genomes,
162 which suggest secondary acquisition by horizontal gene transfer in *D. oryzae* [22,30]. After
163 reclassification of several *D. zeae* strains in the novel species *D. oryzae* [14], the *zms* cluster
164 appeared to be absent in the genomes of true *D. zeae* strains. It is present in some, but not
165 all, *D. oryzae* rice strains (ZYY5, EC1, DZ2Q and ZJU1202) and in only one *D. dadantii* strain
166 (A622-S1-A17). The zeamine biosynthetic clusters from *D. oryzae* EC1 and *D. solani* Ds0432-
167 1 share from 59 to 94% identity at individual protein level [30]. Zeamine-related antibiotics are
168 polyamino-amide molecules toxic to a wide range of pro- and eukaryotic organisms such as
169 bacteria, fungi, oomycetes, plants, and nematodes [31]. Mutation of the zeamine synthase
170 gene *zmsA* in *D. oryzae* EC1 attenuates the inhibition of rice seed germination [24] and
171 suppresses antibacterial activity against *E. coli* [24]. Zeamine produced by *S. plymuthica* kills
172 nematodes and yeast [32]. *D. solani* IPO 2222 can also kill the nematode *Caenorhabditis*
173 *elegans* but not as quickly as *S. plymuthica* [32].
174 To interrupt the synthesis of the secondary molecules produced by these three clusters, we
175 constructed from a Nal^R Gm^R derivative of WT *D. solani* D s0432-1 in-frame deletion mutants
176 inactivating a key gene of each cluster. The inhibitory effects of the mutants Δ*ssmG*, Δ*oocL*
177 and Δ*zmsA* against fungi, bacteria and yeasts were compared with that of the parental strain.
178 To further analyze possible synergistic effects, double mutants Δ*ssmG*Δ*oocL*, Δ*ssmG*Δ*zmsA*
179 and Δ*oocL*Δ*zmsA* as well as the triple mutant (hereafter called Δ3) were also constructed.
180
181 **The *D. solani* oocydin cluster ooc inhibits *Ascomycota* growth, and the *ssm* cluster is**
182 **also involved in the inhibition of some fungi.**
183
184 We compared the ability of the WT *D. solani* strain D s0432-1 and its derived mutants to inhibit
185 the growth of *Botrytis cinerea*, *Magnaporthe oryzae* and *Sclerotinia sclerotiorum*, three fungi-
186 like eukaryotes of the phylum *Ascomycota*. The center of a potato dextrose agar (PDA) plate

187 was inoculated with fungal mycelium, and 5 µl of overnight bacterial culture of each *D. solani*
188 strain grown in M63 minimal medium with sucrose was deposited at the periphery of the plate
189 (Fig. 2). The different *D. solani* strains showed similar overall growth in liquid culture (Fig. S1).
190 After incubation at 25°C for several days, we observed a growth inhibition of the three fungi
191 by the *D. solani* WT and the Δ*ssmG* and Δ*zmsA* mutants. In contrast, the Δ*oocL* mutant
192 seemed less effective: *B. cinerea* and *M. oryzae* mycelium growth was completely unaffected,
193 while a small zone of inhibition was observed for *S. sclerotiorum* (Fig. 2). This suggests that
194 the Δ*oocL* mutant may also produce another molecule that inhibits this fungus. The
195 phenotypes were fully restored in the reverted strain Δ*oocL/oocL*$^{+}$. Double and triple mutants
196 of the secondary metabolite clusters containing the *oocL* deletion showed no differences from
197 the Δ*oocL* mutant with *B. cinerea* and *M. oryzae*. However, the Δ*oocL*Δ*ssmG* double mutant
198 and the Δ3 triple mutant were completely unable to inhibit *S. sclerotiorum* growth (Fig. 2).
199 These data suggest that the *ooc* cluster is mainly responsible for the majority of *Ascomycota*
200 inhibition and that the *ssm* cluster is secondary involved in the inhibition of some fungi. In
201 contrast, the *zms* cluster does not seem to be involved in fungal inhibition.
202
203 **The *D. solani* zeamine cluster inhibits bacterial growth.**

204 The zeamine cluster of *D. oryzae* EC1 is responsible for the a bactericidal activity against
205 *Escherichia coli* DH5α [24]. *D. oryzae* EC1 and *D. solani* zeamine biosynthetic genes share a
206 high degree of similarity [30]. We thus evaluated the capacity of the *D. solani* strain D s0432-
207 1 and its derived mutants to inhibit the growth of gram-positive and gram-negative bacteria
208 (Fig. 3). Only the Δ*zmsA* mutant was unable to inhibit *Bacillus subtilis* growth, indicating that
209 WT *D. solani* produces an active zeamine antibiotic (Fig. 3). The WT phenotype was restored
210 in the reverted Δ*zmsA*/*zmsA*+ strain. We also tested the ability of *D. solani* to inhibit growth of
211 the other gram-positive bacteria *Streptomyces scabiei*, a plant pathogen causing the potato
212 disease common scab [33]. An inhibition of *S. scabiei* growth was observed, except with the
213 Δ*zmsA* mutant. No phenotype difference was observed between the single Δ*zmsA* mutant and

214 the double and triple mutants containing the *zmsA* deletion, suggesting that only the cluster
215 *zms* is required for Gram-positive bacterial growth inhibition. We also tested the ability of *D.*
216 *solani* to inhibit growth of the gram-negative bacteria *E. coli*, *D. dadantii* and *Pectobacterium*
217 *atrosepticum* (Fig. 3). *E. coli* DH5α was, like *B. subtilis* and *S. scabiei*, inhibited by the WT
218 strain through *zms* activity, albeit much less potently (Fig. 3 and Fig. S2). No inhibition of the
219 two other pectinolytic bacteria *D. dadantii* and *P. atrosepticum* growth was observed. In
220 conclusion, out of the three clusters analyzed, only the zeamine-like molecule potentially
221 produced by the *zms* cluster has an anti-bacterial activity against some gram-positive and
222 gram-negative bacteria.

223 **The *D. solani* clusters *ssm* and *zms* inhibits yeast growth.**

224 Since zeamine produced by *S. plymuthica* A153 has previously been shown to be toxic to the
225 ascomycete yeast *Saccharomyces cerevisiae* [32], we tested the capacity of *D. solani* D
226 s0432-1 and its derivative mutant to inhibit the growth of the yeasts *S. cerevisiae*,
227 *Kluyveromyces lactis,* a predominant eukaryote during cheese productions [34], and *Candida*
228 *albicans*, an opportunistic human pathogen. In a growth inhibition assay performed in Yeast
229 Peptone Dextrose (YPD) solid agar medium, we observed a strong inhibition of *K. lactis* by
230 WT *D. solani*, a lower inhibition of *S. cerevisiae*, and a slight inhibition of *C. albicans* (Fig. 4).
231 The Δ*ssmG* mutant was almost completely deficient in its ability to inhibit yeast growth, while
232 the Δ*ssmG*/*ssmG*$^+$ revertant strain showed a restored WT phenotype. The cluster *ssm* is thus
233 primarily responsible for the anti-eukaryotic action against these yeasts (Fig. 4). Nevertheless,
234 a weak halo of inhibition of the yeasts *K. lactis* and *S. cerevisiae* was observable around the
235 mutant Δ*ssmG.* This halo disappeared around the double mutant Δ*ssmG*Δ*zmsA* and the triple
236 mutant Δ*3,* suggesting that the *zms* cluster is also implicated in yeast inhibition, but at a lower
237 level than that observed for the *ssm* cluster. In conclusion, although the zeamine cluster of *D.*
238 *solani* D s0432-1 is involved in the inhibition of yeast growth, as shown for *S. plymuthica* A153
239 [32], *D. solani* D s0432-1 possesses a second cluster *ssm* that produces another anti-yeast
240 molecule.

241 **The WT *D. solani* strains IPO 2222 and IFB0223 are unable to inhibit yeast and bacterial**
242 **growth.**
243 We showed that *D. solani* D s0432-1 has the capacity to inhibit the growth of a wide range of
244 microorganisms, including filamentous fungi, bacteria, and yeasts. We therefore tested
245 whether other WT *D. solani* strains isolated from the environment in Europe, either from
246 lesions of potato tubers or plants, or from potato rhizosphere, possess this ability. We focused
247 our work on *D. solani* strains available in national strain collections and whose genome
248 sequence is available. These strains are D s0432-1, IFB0099, IFB0158, IFB0223, IFB0484,
249 IPO 3337, IPO 3494, IPO 3793 and the *D. solani* type strain IPO 2222. We tested their capacity
250 to inhibit the bacterium *B. subtilis*, the yeast *K. lactis* and the fungus *S. sclerotiorum* (Fig. 5A).
251 All strains were able to inhibit the growth of *S. sclerotiorum*. The inhibition of *B. subtilis* and *K.*
252 *lactis* was clearly observed for all the strains except IPO 2222 and IFB0223. These strong
253 phenotypic differences between IPO 2222 and IFB0223 and the other WT *D. solani* strains
254 could not be explained by any nucleotide variabilities in the *ssm*, *zms*, and *ooc* clusters. All
255 the selected strains carry the *ssm*, *zms*, and *ooc* clusters, with 100% conservation at the
256 nucleotide level (including in the promoter regions). Nonetheless, there are certain changes
257 at the genome level, most notably some nucleotide variability with the presence of SNPs
258 (single-nucleotide polymorphism) and InDel (insertion or deletion), outside the clusters *ssm,*
259 *zms,* and *ooc*. Hence, we searched for variations in the whole genomes by comparing two
260 groups: strains IFB0223 and IPO 2222 that are defective for the growth inhibition of yeast and
261 bacteria, and strains D s0432-1, IPO 3337 and IFB0099 that are efficient for these inhibitions
262 (Table S2).
263 A SNP was observed with an identical nucleotide in the strains D s0432-1, IPO3337 and
264 IFB0099 (a G at position 90 of *arcZ*) but different nucleotide in the strain IPO2222 (a A at
265 position 90 of *arcZ*) (position 2530087 according to IPO 2222 genome). This variation is
266 positioned in the 3' region of the small RNA *arcZ*, known to be a key area interacting with
267 targeted mRNA for post-translational regulation in other bacterial species (Fig. 5C). The ArcZ
268 variants of D s0432-1 and IPO 2222 will be referred to as $ArcZ_1$ and $ArcZ_2$ respectively in the

269 remainder of this article. In the strain IFB0223, we observed a 3-kbp chromosomal deletion
270 covering the gene *arcZ*, and extending between the genes *arcB* and *osmY* (Fig. 5B). In other
271 *D. solani* strains, this region includes *arcZ*, *elbB*, *mtgA*, and a gene encoding an alginate lyase
272 domain (pfam05426). These discoveries led us to hypothesize that the inability of strains
273 IFB0223 and IPO 2222 to inhibit yeast and bacterial growth could be due to an ArcZ deficiency.
274 Before going further, we ordered the *D. solani* IPO 2222 type strain stored in the BCCM
275 collection (LMG25993) to analyse its genotype and phenotype. Using PCR amplification and
276 sanger sequencing of *arcZ,* we confirmed that the *arcZ* allele of LMG 25993 is $arcZ_2$, similarly
277 to the IPO 2222 strain used in our experiments Similarly, the strain IPO 2222 used in our
278 experiments and LMG 25993 have the same inhibition phenotype, i.e., an incapacity to inhibit
279 yeast and bacterial growth (Fig. S3).
280
281 **The *arcZ* gene is required for *zms* and *ssm* anti-microbial activities.**
282 sRNAs are posttranscriptional regulators that most commonly influence gene
283 translation by base-pairing to target mRNAs. In *E. coli*, this regulation often requires the RNA
284 chaperones Hfq or ProQ [35–37]. ArcZ belongs to what is called the “core sRNAs” because it
285 is highly conserved among enterobacterial species [38]. In order to determine if ArcZ is
286 required for secondary metabolite production, the Δ*arcZ* mutants of *D. solani* strains D s0432-
287 1 and IPO 2222 were constructed, and their phenotypes compared to those of the WT strains
288 (Fig. 6A). In M63 sucrose, the mutants grew as well as the parental WT strains (Fig. S4). In
289 our inhibition assay against *B. subtilis* and *K. lactis,* no inhibition zones were observed around
290 the $\Delta arcZ_1$ mutant of D s0432-1 (Fig. 6A), demonstrating that $ArcZ_1$ is required for the
291 synthesis of the metabolites produced from the *ssm* and *zms* clusters in D s0432-1. However,
292 the $\Delta arcZ_1$ mutant of *D. solani* D s0432-1 was still able to inhibit the growth of the fungus *S.*
293 *sclerotiorum*, although a slight decrease in the anti-fungal effect was observed. Thus, ArcZ
294 does not appear to be fully required for *ooc* cluster expression, which is consistent with the
295 results obtained with *D. solani* IFB0223, the naturally *arcZ* deletion mutant capable of inhibiting
296 *S. sclerotiorum* growth (Fig. 5A and Fig. 6A). *D. solani* IPO 2222 WT inhibited neither bacteria

297 nor yeast but inhibited the growth of fungi, and the phenotype of the IPO 2222 Δ*arcZ*$_2$ mutant
298 was similar to that of the IPO 2222 WT or the D s0432-1 Δ*arcZ*$_1$ mutant. This suggests that
299 ArcZ$_2$ might be inactive.
300 To verify the effect of the G90A mutation in *arcZ*, we performed a heterologous
301 complementation experiment by transferring the allele *arcZ*$_1$ from D s0432-1 or *arcZ*$_2$ from IPO
302 2222 in *D. solani* WT strains D s0432-1 or IPO 2222 or their Δ*arcZ* derivatives. The alleles
303 *arcZ*$_1$ and *arcZ*$_2$ were also transferred into *D. solani* IFB0223 naturally deleted for *arcZ*.
304
305 **The G90A mutation in arcZ$_2$ of *D. solani* IPO 2222 causes a loss of function of *zms* and**
306 ***ssm* clusters.**
307 The two allelic forms *arcZ*$_1$ and *arcZ*$_2$ were cloned with their own promoter in the plasmid
308 pWSK29-oriT, a mobilizable low copy plasmid with pSC101 origin and ampicillin resistance
309 gene. DNA sequencing confirmed that the only difference between the two plasmids is the
310 G90A mutation in pWSK29-oriT-*arcZ*$_2$. The recombinant plasmids and the empty vector were
311 transferred by conjugation into WT or Δ*arcZ D. solani* D s0432-1 or IPO 2222 strains, as well
312 as WT *D. solani* IFB0223 (naturally deleted for *arcZ*). The phenotypes of the conjugants were
313 determined by testing their anti-microbial activity against *B. subtilis*, *K. lactis* and *S.*
314 *sclerotiorum* (Fig. 6B).
315 The transfer of *arcZ*$_1$ in Δ*arcZ*$_1$ Ds0432-1 restored the WT phenotypes, proving that the allele
316 *arcZ*$_1$ activates the anti-microbial activities of the *ssm* and *zms* clusters, while the anti-fungal
317 activity was unaffected. In contrast, the transfer of *arcZ*$_2$ in the Δ*arcZ*$_1$ DS0432-1 strain did not
318 restore the WT phenotypes. Thus, the difference in complementation between *arcZ*$_1$ and *arcZ*$_2$
319 is due to the presence of the G90A mutation that impairs ArcZ$_2$ function.
320 An identical result was obtained with the Δ*arcZ*$_2$ mutant of IPO 2222 or the IFB0223 strain
321 carrying the pWSK29-oriT, pWSK29-oriT-*arcZ*$_1$ and pWSK29-oriT-*arcZ*$_2$. Indeed, the transfer
322 of *arcZ*$_1$ in strains WT IPO 2222, Δ*arcZ*$_2$ IPO 2222 or IFB0223 activates the anti-microbial
323 activities of the *ssm* and *zms* clusters. In contrast, the transfer of *arcZ*$_2$ in these strains did not
324 activate the *ssm* and *zms* anti-microbial activities. These data demonstrated that the presence

325 of *arcZ* and the nature of the *arcZ* allele are the main factors governing the difference in
326 phenotypes for antimicrobial activities between the *D. solani* strains D s0432-1 and IPO 2222
327 or IFB0223.
328 Finally, we questioned if an *arcZ* mutation could be found in additional *D. solani* natural
329 isolates. We extended this genomic analysis to 57 *D. solani* genomes, including IPO 2222. It
330 revealed that only four strains have an *arcZ* single-nucleotide mutation, all at different positions
331 in the 3' region of *arcZ*. It is not known whether these other mutations affect the antimicrobial
332 activity of these strains. The *arcZ* DNA sequence of *D. solani* IPO 2222 was also used as a
333 query in a BlastN search against the NCBI nucleotide database. Three *D. fangzhongdai strains*
334 DSM 101947 (CP025003.1), QZH3 (CP031507.1), and LN1 (CP031505.1) had the G90A
335 mutation in *arcZ*. A G90T mutation was also discovered in *D. parazeae* Ech586 (CP001836.1)
336 (Fig. S5). Therefore, the G90 mutation to A or T of *arcZ* can be found in other *Dickeya* species.
337

338 **The G90A mutation in *arcZ*$_2$ of *D. solani* IPO 2222 alters ArcZ$_2$ processing.**

339 To gain further insight into the consequence of the G90A mutation in *arcZ*, Northern-blot
340 experiments were performed to detect the sRNAs ArcZ$_1$ in WT D s0432-1 and ArcZ$_2$ in WT
341 IPO 2222 (Fig. 7). A probe specific to the 3' part of ArcZ$_1$ and ArcZ$_2$ was used (annealing from
342 nucleotide 91 to 132). An abundant smaller transcript (~60nt) representing the processed 3´
343 fragment of ArcZ$_1$ was detected in WT D s0432-1 but not in the mutant D s0432-1 Δ*arcZ*$_1$ (Fig.
344 7, compared lanes 1 and 2). The full-length form corresponding to the ArcZ$_1$ precursor was
345 barely detected. This confirms that the processed form of ArcZ$_1$ is predominant, like observed
346 in *E. coli*, *Salmonella*, and *Photorhabdus* [38–40]. In IPO 2222, only the full-length ArcZ$_2$ was
347 detected in the WT strain whereas no ArcZ$_2$ transcript was detected in the IPO 2222 Δ*arcZ*$_2$
348 mutant (Fig. 7, compared lanes 5 and 6). This result suggests that the G90A mutation present
349 in the allele *arcZ*$_2$ of IPO 2222 prevents ArcZ$_2$ processing in a shorter functional transcript.
350 Next, we wondered if we could relate the importance of ArcZ processing to the activation of
351 the *ssm* and *zms* clusters. To do that, Northern-blot analyses were realized with the *D. solani*

352 Δ*arcZ* strains expressing either the *arcZ*$_1$ or *arcZ*$_2$ allele from the plasmid pWSK29-oriT-*arcZ*.
353 On one hand, Northern blot showed that D s0432-1Δ*arcZ*$_1$, IPO 2222 Δ*arcZ*$_2$ and IFB0223
354 (natural Δ*arcZ*) expressing *arcZ*$_1$ from D s0432-1 accumulate the processed short transcript
355 of ArcZ$_1$ (Fig. 7, lanes 3, 7 and 10) and have the capacity to inhibit yeast and bacteria (Fig. 6).
356 On the other hand, D s0432-1Δ*arcZ*$_1$, IPO 2222 Δ*arcZ*$_2$ and IFB0223 expressing *arcZ*$_2$ from
357 IPO 2222 showed the accumulation of the non-processed transcript of ArcZ$_2$ (Fig. 7, lanes 3,
358 7 and 10) and an inability to inhibit yeast and bacteria (Fig. 6). These results supported the
359 hypothesis that the G90A mutation in ArcZ alters the processing of the ArcZ precursor in a
360 shorter form, leading to its inability to play a correct regulatory function on the *ssm* and *zms*
361 clusters.
362

363 **DISCUSSION**

364 PKS/NRPS secondary metabolite pathways are a great source of molecules with anti-
365 eukaryotic or anti-prokaryotic activity, giving the bacteria that synthesize them a competitive
366 advantage over other organisms. Targeted mutagenesis of the *D. solani* D s0432-1
367 chromosome has allowed us to specifically study the involvement of three secondary
368 metabolite biosynthesis clusters encoded by all the *D. solani* strains for which genome
369 sequence is available. We focused our work on strain D s0432-1, one of the most virulent *D.*
370 *solani* strains [18]. We have demonstrated that *D. solani* D s0432-1 is able to inhibit the growth
371 of a variety of living microorganisms. We tested bio-activities against Gram-negative bacteria
372 (*E. coli*, *P. atrosepticum*, *D. dadantii*), Gram-positive bacteria (*B. subtilis*, *S. scabiei*), yeasts
373 (*S. cerevisiae*, *K. lactis, C. albicans*), and fungi (*B. cinerea*, *M. oryzae* and *S. sclerotiorum*).
374 The cluster *ooc* encodes a biosynthesis pathway that produces an oocydin-like molecule, a
375 chlorinated macrocyclic lactone molecule having antifungal, antioomycete and antitumor
376 activities in *S. plymuthica* [23,29]. It was previously shown that the *D. solani* strains MK10,
377 MK16 and IPO 2222, all encoding the oocydin cluster, inhibit the growth of the fungus *V.*
378 *dahliae* and the oomycete *P. ultimum* [29]. Our study showed that *D. solani* D s0432-1
379 prevents the growth of the fungi *B. cinerea*, *M. oryzae* and *S. sclerotiorum*, and that inactivation

380 of the *oocL* gene suppressed the inhibition of the three fungi without any visible effect on the
381 bacteria or yeasts tested.
382 By testing other mutants of the other secondary metabolite clusters, we showed that the
383 mutant Δ*ssmG* was nearly completely unable of preventing the growth of *S. cerevisiae* and *K.*
384 *lactis*. Therefore, the *ssm* cluster appears to be responsible for yeast inhibition. *D. solani* D
385 s0432-1 also inhibits the human pathogen yeast *C. albicans*, but its inhibitory activity appears
386 to be weaker than that observed with *S. cerevisiae* and *K. lactis* in our inhibition assay. This
387 observation on the *ssm* cluster paves the way for the identification of a new molecule with
388 highly specific inhibitory activity against yeasts. The *ssm* cluster is conserved in several
389 *Dickeya* genomes but rarely in other bacterial genera, except in some *Rouxiella* species. The
390 structure of the molecule and its target remains to be elucidated.
391 Our study also showed that *D. solani* D s0432-1 has an anti-bacterial activity linked to the
392 cluster *zms*, which encodes a zeamine biosynthetic pathway. Zeamine produced by *S.*
393 *plymuthica* kills *B. subtilis,* the yeasts *S. cerevisiae* and *Schizosaccharomyces pombe,* and
394 the nematode *Caenorhabditis elegans* [32]. We showed that *D. solani* D s0432-1, but not the
395 Δ*zmsA* mutant, can clearly inhibit the growth of two Gram-positive bacteria, *B. subtilis* and *S.*
396 *scabies*. Since *D. solani* and *S. scabiei* are two potato pathogens, they might be in competition
397 for the same ecological niche. It is thus interesting to note that *D. solani* can inhibit the growth
398 of another potato pathogen. We also observed a slight inhibition exerted by *D. solani* D s0432-
399 1 against *E. coli*, but no inhibition towards *D. dadantii* and *P. atrosepticum*. Zeamine resistance
400 of *D. dadantii* could be explained by the presence in its genome of the genes *desAB* encoding
401 an RND pump identified in *D. oryzae* EC1 and involved in zeamine efflux [41]. In-frame
402 deletion of *desA* or *desB* in *D. oryzae* EC1 leads to a zeamine sensitive phenotype [41]. In *in*
403 *planta* Tn-seq experiments with *D. dadantii* 3937 [42], mutants of the genes *desA* and *desB*
404 (Dda3937_00787 and Dda3937_00786 respectively) did not display a significant negative or
405 positive variation (Log2 fold-changes -0.09 and +0.44, respectively), suggesting that this RND
406 efflux pump does not play a significant role during *D. dadantii* chicory infection, contrary to the
407 *D. dadantii* RND efflux pump AcrAB that appeared to be essential for virulence [42]. While *P.*

408 *atrosepticum* is not inhibited by *D. solani* D s0432-1, it does not have the genes *desAB*.
409 Zeamine resistance could be provided by another efflux pump or by a different mechanism in
410 *P. atrosepticum*. It's worth remembering that the *D. solani* D s0432-1 Δ*zmsA* mutant grows
411 slightly faster than the WT strain after reaching OD_{600nm} 0.4 (Fig. S1). This small difference in
412 growth might be explained by the lack of need of the mutant to adapt to the presence of
413 zeamine in the medium. We also observed that *D. solani* D s0432-1 Δ*ssmG* produced a very
414 slight halo of inhibition against *S. cerevisiae* and *K. lactis*, barely visible in our tests. This weak
415 halo disappears in the double mutant Δ*ssmG*Δ*zmsA* and the triple mutant
416 Δ*ssmG*Δ*oocL*Δ*zmsA,* showing that the zeamine produced by the *D. solani zms* cluster has
417 also an anti-yeast action. It is worthwhile to remind that zeamine produced by *S. plymuthica*
418 A153 is bioactive against *S. cerevisiae* and *S. pombe* [32].
419 Thus, the presence of three clusters encoding secondary metabolites allows *D. solani* D
420 s0432-1 to produce an arsenal of bioactive secondary metabolites against a variety of living
421 microorganisms. The cluster *ssm* produces an unkown molecule active against yeasts; the
422 cluster *ooc* produces an oocydin-like molecule active against fungi and the cluster *zms*
423 produces a zeamine-like molecule active against bacteria and yeast. In future studies, It would
424 be instructive to investigate *D. solani* behavior toward other organisms found in the
425 environment, such as amoebas, nematodes, or even insects.
426 We then expanded our studies to a larger set of *D. solani* strains isolated in different European
427 countries and years. Through the combination of phenotypic analysis and comparative
428 genomics, confirmed by mutant construction, we demonstrated that the ArcZ sRNA plays a
429 major role in activating the antimicrobial activities of the clusters *ssm* and *zms*. We first
430 observed that some *D. solani* WT strains are defective for yeast inhibition and possess
431 different *arcZ* alleles, a deletion in the case of strain IFB0223, or the presence of a SNP G90A
432 in the 3' part of *arcZ* in the type strain IPO 2222. We demonstrated that these arcZ alterations
433 significantly impair the *D. solani* ability to inhibit other bacteria and yeasts. These *arcZ*-related
434 genomic changes represent a minority of *D. solani* isolates, only two of the nine strains
435 phenotypically tested . Hence, our results show that despite a probable clonal origin,

436 environmental strains of *D. solani* can present very different characteristics due to a single
437 mutation into a regulatory sRNA. The *arcZ* polymorphism may be one of the explanations for
438 the variability of phenotypes and virulence observed between genetically close *D. solani*
439 strains. A global investigation of the polymorphism of all the short RNAs within the genomes
440 of the same species could give surprising results. This study shows that it is critical to pay
441 attention to the allelic diversity due to SNPs present not only in protein coding genes but also
442 in sRNA genes.
443 ArcZ is a well-known regulatory sRNA that is associated with the chaperone Hfq. The ArcZ
444 primary transcript (121 to 134-nt) is converted by the essential endoribonuclease RNAse E
445 [43] to a shorter stable approximative 60-nt RNA retaining the seed region. The precise length
446 of this short processed RNAs depends on the bacterial species [38,40,44,45]. In *E. coli*, the
447 processed short form of ArcZ promotes *rpoS* translation while suppressing the expression of
448 several other genes. In anaerobic conditions, *arcZ* is repressed and translation of RpoS is low
449 [44]. RpoS is the RNA polymerase alternative sigma factor that governs the general stress
450 response, which is activated by a wide range of conditions. It controls 10% of the *E. coli*
451 genome [46]. RpoS can control positively or negatively the production of metabolites such as
452 antibiotics [29,47]. *rpoS* mRNA is not the only ArcZ direct target. In *Photorhabdus* and
453 *Xenorhabdus*, ArcZ pairs with the mRNA encoding HexA, a transcriptional repressor of the
454 expression of specific metabolite gene clusters [40]. In *Dickeya* species, the regulator gene
455 *pecT* is the orthologous gene to *hexA*. In *D. dadantii* 3937, the *pecT* mRNA is also a direct
456 target of ArcZ. Short processed ArcZ binds to Hfq and directly to the 5'UTR region of *pecT*
457 mRNA, repressing its translation [45]. PecT is directly and indirectly involved in the expression
458 of genes encoding plant cell wall degrading enzymes and virulence factors [45]. In the
459 phytopathogen *Erwinia amylovora,* ArcZ participates also in the positive control of T3SS,
460 exopolysaccharide production, biofilm formation, and motility [48]. Finally, another known
461 direct target of ArcZ is the *flhD* mRNA [49,50]. FlhD forms with FlhC the master regulator
462 FlhDC that controls motility in bacteria [51]. Although we demonstrated the critical role of ArcZ
463 in the regulation of secondary metabolite production in *D. solani*, it remains to understand the

464 precise mechanism of ArcZ action on the ssm or zms clusters. We can only speculate that this
465 could occur through the control of *rpoS*, *flhD*, or *pecT*, three regulators known to be ArcZ
466 targets. However, other actors could be involved. Another point to consider is a more global
467 role of *D. solani* ArcZ exerted on other cellular functions such as motility and virulence. ArcZ
468 targets in *D. solani* need to be investigated in the future. It is worth pointing out that the G90
469 nucleotide is in the 3' region of ArcZ that interacts with the target mRNAs *rpoS*, *flhD*, or *pecT*
470 in other bacteria (Fig. S6). Northern-blot analysis revealed that $ArcZ_2$ of *D. solani* IPO 2222 is
471 not processed in the stable shorter sRNA as $ArcZ_1$ of *D. solani* D s0432-1. The G90A mutation
472 in IPO 2222 $ArcZ_2$ is predicted to modify the secondary structure of the ArcZ precursor form
473 (Fig. 7B). Since maturation by RNase E is essential for target regulation by the ArcZ sRNA in
474 *Salmonella*, we conclude that the absence of a short form of ArcZ in IPO 2222 is probably the
475 main cause of the loss of regulatory function of the IPO 2222 $ArcZ_2$.
476 The type strain *D. solani* IPO 2222 is largely used in academic laboratories as a model to
477 study the *D. solani* species. In light of our findings, it could be important to compare data
478 obtained with the strain IPO 2222 with those obtained with other *D. solani* strains. The *arcZ*
479 mutations may be responsible, at least partially, for the lower virulence of IPO 2222 and
480 IFB0223 observed previously in comparison to D s0432-1 [18]. Even strains with the same
481 *arcZ*, *ssm*, *ooc*, and *zms* genomic sequences as D s0432-1, showed heterogeneity in their
482 ability to inhibit other micro-organisms. For example, IPO 3494 and IFB0484 inhibited *B.*
483 *subtilis* better than other *D. solani* strains (Fig. 5A). Other specific mutations in the genomes
484 of these strains, which could also modify the activity of secondary metabolite clusters, could
485 explain these phenotypic variations.
486 We first described the inhibitory function of the *ssm* cluster of the *D. solani* strain D s0432-1
487 against the yeasts *S. cerevisiae* and *K. lactis* in a 2021 bioRxiv preprint [27]. Very recently, in
488 November 2022, Matilla *et al.* published results on the *ssm* cluster of the *D. solani* strain MK10
489 [26]. The *ssm* cluster was named *sol* in this study and the authors described the antifungal
490 activity of the uncharacterized molecule that they called solanimycin [26]. Matilla *et al.* also
491 report the inhibition observed with the *D. solani* strain IPO 2222 against *Verticillium dahliae*

492 and *Schizosaccharomyces pombe* ([26], Fig S1). In our conditions, strain IPO 2222 was able
493 to inhibit the fungus *Sclerotinia sclerotiorum* but not the yeast *Kluyveromyces lactis* (Fig. 5).
494 In comparison to our study, Matilla *et al* used different fungal species but also different growth
495 conditions (medium, temperature, exposure time, etc). By random mutagenesis of strain
496 MK10, they identified RsmA and the two *Dickeya* quorum-sensing systems ExpI/R and Vfm
497 as regulators of the *ssm/sol* cluster such [26]. Interestingly, the Rsm regulatory pathway of *D.*
498 *dadantii* 3937 is regulated by PecT, which is under the ArcZ control [45]. Further studies are
499 now necessary to specify the biological targets of solanimycin and to clarify the role in *ssm/sol*
500 expression of the sRNA ArcZ, quorum-sensing, and transcriptional regulators PecT or RsmA,
501 in order to better understand the regulatory network controlling the production of secondary
502 metabolites in *D. solani*. Our lab is currently investigating the regulatory pathway of secondary
503 metabolite clusters from ArcZ.
504 In conclusion, our results provide the basis for further investigation of a novel metabolite
505 capable of limiting yeast growth and, at the same time, open doors to understand how the
506 ArcZ sRNA acts as a global regulator to regulate two different clusters of secondary
507 metabolites in *D. solani*. It also shows how a single mutation in a small RNA can greatly modify
508 the phenotype of bacterial strains that are very close phylogenetically.
509

510 **MATERIAL AND METHODS**

511 **Bacterial and fungal strains, plasmids and growth conditions.**

512 The *E. coli* and *Dickeya* bacterial strains, plasmids and oligonucleotides used in this study are
513 described in Table S3 and S4. The genome accession number of *D. solani* D s0432-1 is
514 NZ_CP017453. The following strains have been used in the study: *Sclerotinia sclerotiorum*
515 S5, *Botrytis cinerea* B05.10, *Magnaporthe oryzae* Guy11, *Saccharomyces cerevisiae* BY4743
516 (*MATa/α his3Δ1/his3Δ1 leu2Δ0/leu2Δ0 LYS2/lys2Δ0 met15Δ0/MET15 ura3Δ0/ura3Δ0)*,
517 *Kluyveromyces lactis* MWL9S1 [52], *Candida albicans* SC5314, *Dickeya dadantii* 3937,
518 *Pectobacterium atrosepticum* SCRI1043*, Streptomyces scabiei* CFBP4517, *Bacillus subtilis*
519 PY79. *E. coli* was grown routinely at 37°C in LB. Fungus strains were grown at 25°C onto

520 Potato Dextrose Agar (PDA). *S. scabiei* was grown in tryptic soy broth (TSB) medium at 28°C.
521 *B. subtilis*, *P. atrosepticum* and the *Dickeya* strains were cultivated in LB unless specified.
522 Yeast cells were grown at 30°C in rich medium consisting of complete yeast extract-peptone
523 (YP) medium containing 1% Bacto yeast extract, 1% Bacto peptone (Difco) supplemented with
524 2% glucose (yeast extract-peptone-dextrose [YPD] medium). For the bacteria, yeast and fungi
525 inhibition assay, M63 medium supplemented with sucrose (2 g $(NH_4)_2SO_4$, 13.6 g KH_2PO_4, 2.5
526 mg $FeSO_47H_2O$, 0.2 g $MgSO_47H_2O$, 10 g sucrose, per liter) were employed to grow overnight
527 the *D. solani* strains before performing the assay.
528 When required, antibiotics were added at the following concentrations: ampicillin (Amp), 100
529 µg/L; nalidixic acid (Nal), 10 µg/mL. Diaminopimelic acid (DAP) (57 µg/mL) was added for the
530 growth of the *E. coli* MFDpir strain. Media were solidified with 12 g/L agar.
531
532 **Growth inhibition assay of bacteria and yeast.**
533 *D. solani* strains were grown for 24 h at 30°C with shaking in M63 medium supplemented with
534 1% sucrose. *B. subtilis*, *E. coli*, *D. dadantii* and *P. atrosepticum* were grown in LB at 30°C with
535 shaking overnight. The next day, the OD_{600} of the cultures of *D. solani* were adjusted to 2. The
536 temperature of melted LB agar was lowered to around 40°C (just before the agar re-solidified).
537 100 mL of the LB agar in surfusion were mixed with 100 µl of the OD_{600} 1 culture of *B. subtilis*,
538 *E. coli*, *D. dadantii* or *P. atrosepticum*. 30 mL of inoculated LB agar were poured in 12- by 12-
539 cm square plates. Then 5 µl of the OD_{600} 2 cultures of *D. solani* were spotted onto the
540 inoculated square plates which were incubated at 30°C for 24-48 h before visualization of the
541 inhibition zone.
542 The same experiment was conducted with *S. scabiei*, except that it was grown for 3 days in
543 TSB at 28°C and TSB agar was poured in the square plates. With the yeasts *S. cerevisiae*, *K.*
544 *lactis*, and *C. albicans*, a similar protocol was used with YPD medium and with OD_{600} 2 culture
545 of yeast per 30mL of medium.
546
547 **Growth inhibition of fungal strains.**

548 *S. sclerotiorum*, *B. cinerea* and *M. oryzae* were grown onto PDA plates at 25°C for 5, 7 and
549 10 days respectively. *D. solani* strains were grown for 24 h at 30°C with shaking in M63
550 medium supplemented with 1% sucrose. The OD_{600} of these overnight cultures were adjusted
551 to 2. Then, 5 µl of the bacterial suspensions were spotted onto PDA plates with 5 mm agar
552 plugs of fungus at the center of the Petri dish. The radius of fungus inhibition zone was
553 measured.
554
555 **Construction of the MLSA tree positioning strains within the *Dickeya* genus.**
556 Details on the methods used for the construction of MLSA tree positioning strains are given in
557 Supplementary Material and Methods.
558
559 **Constructions of the mutant strains and plasmids**
560 All the material and methods for the construction of the strains and plasmids used in this study
561 are given in Supplementary Material and Methods.
562
563 **RNA isolation and Northern detection**
564 All the material and methods for RNA isolation and Northern detection performed in this study
565 are given in Supplementary Material and Methods.
566
567 **ACKNOWLEDGMENTS**
568 B.T. was supported by a PhD grant from the Ministère de l'Enseignement Supérieur, de la
569 Recherche et de l'Innovation. We thank Veronique Utzinger for technical assistance, the
570 members of the Membrane Trafficking and Signaling in Bacteria (MTSB) team for discussions,
571 Amélie De Vallée, Nathalie Poussereau and Christophe Bruel for advices on fungi growth and
572 providing the strains, Alexandre Soulard, Marc Lemaire and Jade Ravent for advices on yeast
573 growth and providing the strains and medium. We would also like to thank the past reviewers
574 whose comments allowed us to greatly improve this study.
575

576 **AUTHOR CONTRIBUTION**

577 B.T., E.G. B.J. A.L., G.C., C.J., G.E carried out the experiments. G.E wrote the manuscript
578 with support from B.T, E.G., A.L., R.M., F.D. and H-C-P.N.
579 F.D., C.J. H-C-P.N. and R.M. performed the phylogenetic and bioinformatic analyses. G.E
580 conceived the original idea with advises from H-C-P.N. G.E supervised the project. All authors
581 provided critical feedback and helped shape the research, analysis and manuscript.

582

583 **CONFLICT OF INTEREST**

584 The authors state that the research was conducted in the absence of any commercial or
585 financial relationship that could be interpreted as a potential conflict of interest.

586

587 **FUNDING**

588 This work was supported by a grant from Agence Nationale de la Recherche to L.A. (Project
589 RNAchap, ANR-17-CE11-0009-01) and to E.G. (Project Tn-Phyto, ANR- 19-CE35-0016). E.G
590 was also supported by the FR BioEEnVis, annual credits from the University Lyon I and the
591 CNRS at regular basis.

592

593 **REFERENCES**

594 1. Hugouvieux-Cotte-Pattat N, Condemine G, Gueguen E, Shevchik VE. Dickeya Plant
595 Pathogens. eLS. American Cancer Society; 2020. pp. 1–10.
596 doi:10.1002/9780470015902.a0028932

597 2. Charkowski A, Blanco C, Condemine G, Expert D, Franza T, Hayes C, et al. The role of
598 secretion systems and small molecules in soft-rot Enterobacteriaceae pathogenicity.
599 Annu Rev Phytopathol. 2012;50: 425–449. doi:10.1146/annurev-phyto-081211-173013

600 3. Van Gijsegem F, Toth IK, van der Wolf JM. Soft Rot Pectobacteriaceae: A Brief
601 Overview. In: Van Gijsegem F, van der Wolf JM, Toth IK, editors. Plant Diseases
602 Caused by Dickeya and Pectobacterium Species. Cham: Springer International
603 Publishing; 2021. pp. 1–11. doi:10.1007/978-3-030-61459-1_1

604 4. Hugouvieux-Cotte-Pattat N, Condemine G, Shevchik VE. Bacterial pectate lyases,
605 structural and functional diversity. Environ Microbiol Rep. 2014;6: 427–440.

606 5. Samson R, Legendre JB, Christen R, Saux MF-L, Achouak W, Gardan L. Transfer of
607 Pectobacterium chrysanthemi (Burkholder et al. 1953) Brenner et al. 1973 and
608 Brenneria paradisiaca to the genus Dickeya gen. nov. as Dickeya chrysanthemi comb.

nov. and Dickeya paradisiaca comb. nov. and delineation of four novel species, Dickeya dadantii sp. nov., Dickeya dianthicola sp. nov., Dickeya dieffenbachiae sp. nov. and Dickeya zeae sp. nov. Int J Syst Evol Microbiol. 2005;55: 1415–1427. doi:10.1099/ijs.0.02791-0

6. Hugouvieux-Cotte-Pattat N, Van Gijsegem F. Diversity within the Dickeya zeae complex, identification of Dickeya zeae and Dickeya oryzae members, proposal of the novel species Dickeya parazeae sp. nov. Int J Syst Evol Microbiol. 2021;71. doi:10.1099/ijsem.0.005059

7. Brady CL, Cleenwerck I, Denman S, Venter SN, Rodríguez-Palenzuela P, Coutinho TA, et al. Proposal to reclassify Brenneria quercina (Hildebrand and Schroth 1967) Hauben et al. 1999 into a new genus, Lonsdalea gen. nov., as Lonsdalea quercina comb. nov., descriptions of Lonsdalea quercina subsp. quercina comb. nov., Lonsdalea quercina subsp. iberica subsp. nov. and Lonsdalea quercina subsp. britannica subsp. nov., emendation of the description of the genus Brenneria, reclassification of Dickeya dieffenbachiae as Dickeya dadantii subsp. dieffenbachiae comb. nov., and emendation of the description of Dickeya dadantii. Int J Syst Evol Microbiol. 2012;62: 1592–1602. doi:10.1099/ijs.0.035055-0

8. Parkinson N, DeVos P, Pirhonen M, Elphinstone J. Dickeya aquatica sp. nov., isolated from waterways. Int J Syst Evol Microbiol. 2014;64: 2264–2266. doi:10.1099/ijs.0.058693-0

9. van der Wolf JM, Nijhuis EH, Kowalewska MJ, Saddler GS, Parkinson N, Elphinstone JG, et al. Dickeya solani sp. nov., a pectinolytic plant-pathogenic bacterium isolated from potato (Solanum tuberosum). Int J Syst Evol Microbiol. 2014;64: 768–774. doi:10.1099/ijs.0.052944-0

10. Tian Y, Zhao Y, Yuan X, Yi J, Fan J, Xu Z, et al. Dickeyafangzhongdai sp. nov., a plant-pathogenic bacterium isolated from pear trees (Pyrus pyrifolia). Int J Syst Evol Microbiol. 2016;66: 2831–2835. doi:10.1099/ijsem.0.001060

11. Hugouvieux-Cotte-Pattat N, Jacot-des-Combes C, Briolay J. Dickeya lacustris sp. nov., a water-living pectinolytic bacterium isolated from lakes in France. Int J Syst Evol Microbiol. 2019;69: 721–726. doi:10.1099/ijsem.0.003208

12. Hugouvieux-Cotte-Pattat N, Brochier-Armanet C, Flandrois J-P, Reverchon S. Dickeya poaceiphila sp. nov., a plant-pathogenic bacterium isolated from sugar cane (Saccharum officinarum). Int J Syst Evol Microbiol. 2020;70: 4508–4514. doi:10.1099/ijsem.0.004306

13. Oulghazi S, Pédron J, Cigna J, Lau YY, Moumni M, Van Gijsegem F, et al. Dickeya undicola sp. nov., a novel species for pectinolytic isolates from surface waters in Europe and Asia. Int J Syst Evol Microbiol. 2019;69: 2440–2444. doi:10.1099/ijsem.0.003497

14. Wang X, He S-W, Guo H-B, Han J-G, Thin KK, Gao J-S, et al. Dickeya oryzae sp. nov., isolated from the roots of rice. Int J Syst Evol Microbiol. 2020;70: 4171–4178. doi:10.1099/ijsem.0.004265

15. Blin P, Robic K, Khayi S, Cigna J, Munier E, Dewaegeneire P, et al. Pattern and causes of the establishment of the invasive bacterial potato pathogen Dickeya solani and of the maintenance of the resident pathogen D. dianthicola. Mol Ecol. 2021;30: 608–624. doi:https://doi.org/10.1111/mec.15751

654 16. Garlant L, Koskinen P, Rouhiainen L, Laine P, Paulin L, Auvinen P, et al. Genome
655 Sequence of Dickeya solani, a New soft Rot Pathogen of Potato, Suggests its
656 Emergence May Be Related to a Novel Combination of Non-Ribosomal
657 Peptide/Polyketide Synthetase Clusters. Diversity. 2013;5: 824–842.
658 doi:10.3390/d5040824

659 17. Pédron J, Mondy S, des Essarts YR, Van Gijsegem F, Faure D. Genomic and
660 metabolic comparison with Dickeya dadantii 3937 reveals the emerging Dickeya solani
661 potato pathogen to display distinctive metabolic activities and T5SS/T6SS-related toxin
662 repertoire. BMC Genomics. 2014;15: 283. doi:10.1186/1471-2164-15-283

663 18. Golanowska M, Potrykus M, Motyka-Pomagruk A, Kabza M, Bacci G, Galardini M, et al.
664 Comparison of Highly and Weakly Virulent Dickeya solani Strains, With a View on the
665 Pangenome and Panregulon of This Species. Front Microbiol. 2018;9: 1940.
666 doi:10.3389/fmicb.2018.01940

667 19. Motyka-Pomagruk A, Zoledowska S, Misztak AE, Sledz W, Mengoni A, Lojkowska E.
668 Comparative genomics and pangenome-oriented studies reveal high homogeneity of
669 the agronomically relevant enterobacterial plant pathogen Dickeya solani. BMC
670 Genomics. 2020;21: 449. doi:10.1186/s12864-020-06863-w

671 20. Khayi S, Blin P, Pédron J, Chong T-M, Chan K-G, Moumni M, et al. Population
672 genomics reveals additive and replacing horizontal gene transfers in the emerging
673 pathogen Dickeya solani. BMC Genomics. 2015;16: 788. doi:10.1186/s12864-015-
674 1997-z

675 21. Cane DE, Walsh CT. The parallel and convergent universes of polyketide synthases
676 and nonribosomal peptide synthetases. Chem Biol. 1999;6: R319–R325.
677 doi:10.1016/S1074-5521(00)80001-0

678 22. Duprey A, Taib N, Leonard S, Garin T, Flandrois JP, Nasser W, et al. The
679 phytopathogenic nature of Dickeya aquatica 174/2 and the dynamic early evolution of
680 Dickeya pathogenicity. Environ Microbiol. 2019;21: 2809–2835. doi:10.1111/1462-
681 2920.14627

682 23. Matilla MA, Stöckmann H, Leeper FJ, Salmond GPC. Bacterial Biosynthetic Gene
683 Clusters Encoding the Anti-cancer Haterumalide Class of Molecules. J Biol Chem.
684 2012;287: 39125–39138. doi:10.1074/jbc.M112.401026

685 24. Zhou J, Zhang H, Wu J, Liu Q, Xi P, Lee J, et al. A Novel Multidomain Polyketide
686 Synthase Is Essential for Zeamine Production and the Virulence of Dickeya zeae. Mol
687 Plant-Microbe Interactions®. 2011;24: 1156–1164. doi:10.1094/MPMI-04-11-0087

688 25. Masschelein J, Mattheus W, Gao L-J, Moons P, Houdt RV, Uytterhoeven B, et al. A
689 PKS/NRPS/FAS Hybrid Gene Cluster from Serratia plymuthica RVH1 Encoding the
690 Biosynthesis of Three Broad Spectrum, Zeamine-Related Antibiotics. PLOS ONE.
691 2013;8: e54143. doi:10.1371/journal.pone.0054143

692 26. Matilla MA, Monson RE, Murphy A, Schicketanz M, Rawlinson A, Duncan C, et al.
693 Solanimycin: Biosynthesis and Distribution of a New Antifungal Antibiotic Regulated by
694 Two Quorum-Sensing Systems. Sperandio V, editor. mBio. 2022; e02472-22.
695 doi:10.1128/mbio.02472-22

696 27. Effantin G, Brual T, Rahbé Y, Hugouvieux-Cotte-Pattat N, Gueguen E. Dickeya solani
697 D s0432-1 produces an arsenal of secondary metabolites with anti-prokaryotic and anti-

698 eukaryotic activities against bacteria, yeasts, fungi, and aphids. bioRxiv; 2021. p.
699 2021.07.19.452942. doi:10.1101/2021.07.19.452942

700 28. Strobel G, Li J-Y, Sugawara F, Koshino H, Harper J, Hess WM. Oocydin A, a
701 chlorinated macrocyclic lactone with potent anti- oomycete activity from Serratia
702 marcescens. Microbiology. 1999;145: 3557–3564. doi:10.1099/00221287-145-12-3557

703 29. Matilla MA, Leeper FJ, Salmond GPC. Biosynthesis of the antifungal haterumalide,
704 oocydin A, in Serratia, and its regulation by quorum sensing, RpoS and Hfq. Environ
705 Microbiol. 2015;17: 2993–3008. doi:10.1111/1462-2920.12839

706 30. Zhou J, Cheng Y, Lv M, Liao L, Chen Y, Gu Y, et al. The complete genome sequence
707 of Dickeya zeae EC1 reveals substantial divergence from other Dickeya strains and
708 species. BMC Genomics. 2015;16: 571. doi:10.1186/s12864-015-1545-x

709 31. Masschelein J, Jenner M, Challis GL. Antibiotics from Gram-negative bacteria: a
710 comprehensive overview and selected biosynthetic highlights. Nat Prod Rep. 2017;34:
711 712–783. doi:10.1039/C7NP00010C

712 32. Hellberg JEEU, Matilla MA, Salmond GPC. The broad-spectrum antibiotic, zeamine,
713 kills the nematode worm Caenorhabditis elegans. Front Microbiol. 2015;6.
714 doi:10.3389/fmicb.2015.00137

715 33. Loria R, Kers J, Joshi M. Evolution of Plant Pathogenicity in Streptomyces. Annu Rev
716 Phytopathol. 2006;44: 469–487. doi:10.1146/annurev.phyto.44.032905.091147

717 34. Rodicio R, Heinisch JJ. Yeast on the milky way: genetics, physiology and biotechnology
718 of Kluyveromyces lactis. Yeast. 2013;30: 165–177. doi:https://doi.org/10.1002/yea.2954

719 35. Valentin-Hansen P, Eriksen M, Udesen C. MicroReview: The bacterial Sm-like protein
720 Hfq: a key player in RNA transactions. Mol Microbiol. 2004;51: 1525–1533.
721 doi:10.1111/j.1365-2958.2003.03935.x

722 36. Vogel J, Luisi BF. Hfq and its constellation of RNA. Nat Rev Microbiol. 2011;9: 578–
723 589. doi:10.1038/nrmicro2615

724 37. Dutta T, Srivastava S. Small RNA-mediated regulation in bacteria: A growing palette of
725 diverse mechanisms. Gene. 2018;656: 60–72. doi:10.1016/j.gene.2018.02.068

726 38. Papenfort K, Said N, Welsink T, Lucchini S, Hinton JCD, Vogel J. Specific and
727 pleiotropic patterns of mRNA regulation by ArcZ, a conserved, Hfq-dependent small
728 RNA. Mol Microbiol. 2009;74: 139–158. doi:10.1111/j.1365-2958.2009.06857.x

729 39. Argaman L, Hershberg R, Vogel J, Bejerano G, Wagner EGH, Margalit H, et al. Novel
730 small RNA-encoding genes in the intergenic regions of Escherichia coli. Curr Biol.
731 2001;11: 941–950. doi:10.1016/S0960-9822(01)00270-6

732 40. Neubacher N, Tobias NJ, Huber M, Cai X, Glatter T, Pidot SJ, et al. Symbiosis,
733 virulence and natural-product biosynthesis in entomopathogenic bacteria are regulated
734 by a small RNA. Nat Microbiol. 2020;5: 1481–1489. doi:10.1038/s41564-020-00797-5

735 41. Liang Z, Huang L, He F, Zhou X, Shi Z, Zhou J, et al. A Substrate-Activated Efflux
736 Pump, DesABC, Confers Zeamine Resistance to Dickeya zeae. mBio. 2019;10.
737 doi:10.1128/mBio.00713-19

738 42. Royet K, Parisot N, Rodrigue A, Gueguen E, Condemine G. Identification by Tn-seq of
739 Dickeya dadantii genes required for survival in chicory plants. Mol Plant Pathol.
740 2019;20: 287–306. doi:10.1111/mpp.12754

741 43. Chao Y, Li L, Girodat D, Förstner KU, Said N, Corcoran C, et al. In Vivo Cleavage Map
742 Illuminates the Central Role of RNase E in Coding and Non-coding RNA Pathways. Mol
743 Cell. 2017;65: 39–51. doi:10.1016/j.molcel.2016.11.002

744 44. Mandin P, Gottesman S. Integrating anaerobic/aerobic sensing and the general stress
745 response through the ArcZ small RNA. EMBO J. 2010;29: 3094–3107.
746 doi:10.1038/emboj.2010.179

747 45. Yuan X, Zeng Q, Khokhani D, Tian F, Severin GB, Waters CM, et al. A feed-forward
748 signalling circuit controls bacterial virulence through linking cyclic di-GMP and two
749 mechanistically distinct sRNAs, ArcZ and RsmB. Environ Microbiol. 2019;21: 2755–
750 2771. doi:10.1111/1462-2920.14603

751 46. Battesti A, Majdalani N, Gottesman S. The RpoS-mediated general stress response in
752 Escherichia coli. Annu Rev Microbiol. 2011;65: 189–213. doi:10.1146/annurev-micro-
753 090110-102946

754 47. Wilf NM, Salmond GPC. The stationary phase sigma factor, RpoS, regulates the
755 production of a carbapenem antibiotic, a bioactive prodigiosin and virulence in the
756 enterobacterial pathogen Serratia sp. ATCC 39006. Microbiology. 2012;158: 648–658.
757 doi:10.1099/mic.0.055780-0

758 48. Zeng Q, McNally RR, Sundin GW. Global Small RNA Chaperone Hfq and Regulatory
759 Small RNAs Are Important Virulence Regulators in Erwinia amylovora. J Bacteriol.
760 2013;195: 1706–1717. doi:10.1128/JB.02056-12

761 49. De Lay N, Gottesman S. A complex network of small non-coding RNAs regulate motility
762 in Escherichia coli. Mol Microbiol. 2012;86: 524–538. doi:10.1111/j.1365-
763 2958.2012.08209.x

764 50. Schachterle JK, Zeng Q, Sundin GW. Three Hfq-dependent small RNAs regulate
765 flagellar motility in the fire blight pathogen Erwinia amylovora. Mol Microbiol. 2019;111:
766 1476–1492. doi:10.1111/mmi.14232

767 51. Fraser GM, Hughes C. Swarming motility. Curr Opin Microbiol. 1999;2: 630–635.
768 doi:10.1016/S1369-5274(99)00033-8

769 52. Wésolowski-Louvel M. An efficient method to optimize Kluyveromyces lactis gene
770 targeting. FEMS Yeast Res. 2011;11: 509–513. doi:10.1111/j.1567-1364.2011.00741.x

771 53. Clamp M, Cuff J, Searle SM, Barton GJ. The Jalview Java alignment editor. Bioinforma
772 Oxf Engl. 2004;20: 426–427. doi:10.1093/bioinformatics/btg430

773 54. Edgar RC. MUSCLE: a multiple sequence alignment method with reduced time and
774 space complexity. BMC Bioinformatics. 2004;5: 113. doi:10.1186/1471-2105-5-113

775

776

777

778

779

780

781 **FIGURE LEGENDS**

782

783 **<u>Figure 1</u>. Organization and distribution of the secondary metabolite clusters *ssm*, *ooc*,**
784 **and *zms* of *D. solani* D s0432-1.**

785 (A) Organization of the clusters *ssm*, *ooc*, and *zms*. Genes are indicated using the NCBI
786 nomenclature of the NCBI reference genome sequence NZ_CP017453.1 of *D. solani* D s0432-
787 1. XXXXX are the digital number in BJD21_RSXXXXX, which corresponds to the locus tag.
788 Arrowheads show gene orientations. Color code indicates gene function. The red-framed
789 arrows indicate genes targeted for in-frame deletion performed in this study. (B) MLSA tree
790 positioning strains within the *Dickeya* genus. The evolutionary history was inferred by using
791 the Maximum Likelihood method. The presence (green frame) or absence (red frame) of the
792 cluster *ssm*, *ooc*, and *zms* are indicated in front of each strain. The distribution of these clusters
793 in 155 *Dickeya* strains whose genome has been sequenced is given in Table S1.

794

795 **<u>Figure 2</u>. Inhibition of fungal growth by *D. solani* Ds0432-1 and mutant derivatives.**
796 5 µL of bacteria culture at OD_{600nm}= 2 from *D. solani* Ds0432-1 (WT) or derivatives were
797 spotted onto PDA plates inoculated with plugs of *S. sclerotiorum, B. cinerea or M. oryzae*
798 *mycelium.* Plates were incubated at 25°C until the mycelium covers the plate. Lengths of fungi
799 inhibition zone were measured in 4 independent experiments. A statistical difference was
800 significant only between the WT and Δ*oocL* mutants (Mann-Whitney test; * p-value < 0.05).

801

802 **<u>Figure 3</u>. Inhibition of bacteria by *D. solani* Ds0432-1 and mutant derivatives.**
803 Bioassay plates were prepared by mixing bacterial culture (*B. subtilis, S. scabiei, E. coli, D.*
804 *dadantii and P. atrosepticum*) with warm LB agar. 5 µL of bacterial cultures at OD_{600nm}= 2 from

805 *D. solani* Ds0432-1 (WT) or derivatives were spotted onto the plate and incubation was
806 performed at 30°C during 48 h. A slight inhibition zone was observed with *B. subtilis* and *E.*
807 *coli*, except with the *Δzms* mutants. All experiments were carried in 4 replicates.
808
809 **Figure 4. Inhibition of yeasts by *D. solani* Ds0432-1 and mutant derivatives.**
810 Bioassay plates were prepared by mixing yeast culture (*S. cerevisiae, K. lactis, C. albicans*)
811 with warm YPD agar. (A) 5 µL of bacterial culture at OD_{600nm}= 2 from *D. solani* Ds0432-1 (WT)
812 or derivatives were spotted onto the plates and incubation was performed at 30°C during 48
813 h. (B) The radius of each inhibition zone was measured. A statistical difference was significant
814 only between the WT and the *Δssm* mutants (Mann-Whitney test; * p-value < 0.05). For *C.*
815 *albicans,* the inhibition zone was too small to be quantified. All experiments were carried in 4
816 replicates.
817
818 **Figure 5. *D. solani* WT strains deficient for anti-microbial activity are mutated for the**
819 **sRNA *arcZ*.**
820 (A) Inhibition of *B. subtilis*, *K. lactis* and S. *sclerotiorum* by diverse WT *D. solani* strains. The
821 tests were performed as previously described using the nine strains IFB 0099
822 (NZ_CP024711), IFB 0158 (NZ_PENA00000000), IFB 0223 (NZ_CP024710), D s0432-1
823 (NZ_CP017453), IPO 3494 (NZ_CM001842), IFB 0484 (NZ_CM001860), IPO 3337
824 (NZ_CP016928), IPO 3793 (NZ_CP017454) or the type strain IPO 2222 (NZ_CP015137).
825 Only IFB 0223 and IPO 2222 were unable to inhibit *B. subtilis* and *K. lactis.* (B) Organization
826 and conservation of the *arcZ* locus in the nine *D. solani* strains. The single mutation G90A in
827 IPO 2222 *arcZ* is symbolized by a dark spot in the red *arcZ* arrow. (C) Zoom on the nucleotide
828 sequence around *arcZ* of *D. solani* D s0432-1. This allele is named $arcZ_1$. Positions and
829 orientations of the genes *elbB*, *arcZ* and *arcB* are indicated. The location of the G90A mutation
830 present in IPO 2222 is indicated. This allele is named $arcZ_2$.
831
832 **Figure 6: Inhibition of *K. lactis* and *B. subtilis* by *D. solani* is regulated by ArcZ.**

833 Yeast bioassay plates were prepared by mixing culture of *K. lactis* with warm YPD agar.
834 Bacteria bioassay plates were prepared by mixing culture of *B. subtilis* with warm LB agar.
835 PDA plates were inoculated with plugs of *S. sclerotiorum.* For each experiment, 5 µL of
836 bacterial culture at OD_{600nm}=2 from the different *D. solani* strains were spotted onto the plate.
837 (A) Inhibition zones observed with Ds0432-1, IPO 2222, their respective Δ*arcZ* mutants and
838 IFBO223. $ArcZ_1$ is required for the synthesis of metabolites produced by the clusters *ssm* and
839 *zms* (inhibition of *K. lactis* and *B. subtilis*, respectively) but not for the metabolite produced by
840 the cluster *ooc* (inhibition of *S. sclerotiorum*). (B) Complementation tests and heterologous
841 expression of the alleles *arcZ*1 or *arcZ*2 in the three *D. solani* strains. $ArcZ_1$ activates the anti-
842 microbial activities of *ssm* and *zms* clusters in IPO 2222 and IFBO223. All experiments were
843 carried in 4 replicates.
844
845 **<u>Figure 7</u>. Expression of different ArcZ alleles: the G90A mutation in $ArcZ_2$ does not**
846 **prevent its production but its processing**
847 (A) Detection of the sRNA $ArcZ_1$ and $ArcZ_2$ by Northern Blot in *D. solani* strains. A small
848 transcript (~60 nt) corresponding to the processed 3´ fragment of $ArcZ_1$ was detected in D
849 s0432-1 and in all strains expressiong *$arcZ_1$* on plasmid. In IPO 2222, only the full-length form
850 (~132nt) $ArcZ_2$ was detected, as well as in strains expressing the allele *$arcZ_2$* on plasmid. The
851 5S RNA is used as a loading control. This experiment was performed twice with biological
852 replicates and gave identical results. (B) Prediction of secondary structure of the precursor
853 forms of $ArcZ_1$ and $ArcZ_2$ by RNA fold. Bases are colored according to base-pairing
854 probabilities (see color scale). The G90A mutation present in $ArcZ_2$ seems to modify the
855 structure of the ArcZ sRNA precursor.
856
857 **<u>Figure S1</u>. Growth curves of *D. solani* strains and mutant derivatives.**
858 A 96-well plate containing M63 medium with 1% sucrose was inoculated with the strains used
859 in this study at an OD of 0.06. The growth of each strain was determined by measuring OD_{600}

860 every 20 minutes during 2 days in TECAN. The different strains showed similar overall growth,
861 except for the light grey points where a low but significant fitness gain was observed for the
862 mutants Δ*zms,* Δ*ssm* Δ*zms,* Δ*ooc* Δ*zms* and Δ*ssm* Δ*ooc* Δ*zms* (Mann-Whitney test, p-
863 value<0.05).
864
865 **<u>Figure S2</u>. Inhibition of *E. coli* growth by *D. solani* D s0432-1 and mutant derivatives**
866 **(zoom on drop borders).**
867 Bioassay plates were prepared by mixing *E. coli* culture with melted LB agar as described in
868 experimental procedures. 5 µL of bacterial culture at OD_{600nm} = 2 of *D. solani* D s0432-1 (WT)
869 or derivatives were spotted onto the plate and incubated at 30°C during 48 h. A slight inhibition
870 zone was observed except with the Δ*zms* mutant. All experiments were carried in 4 replicates.
871
872 **<u>Figure S3</u>. Phenotypes and *arcZ* sequence of WT *D. solani* IPO 2222 from the BCCM**
873 **collection (LMG 25993).**
874 **(**A) Inhibition assay of *K. lactis, B. subtilis* and *S. sclerotiorum* by WT *D. solani* IPO 2222 LMG
875 25993 from BCCM collection, compared to the strains used in this study. (B) Sanger
876 sequencing results of *D. solani* IPO 2222 *arcZ* (LMG 25993). The mutation G90A is highlighted
877 by a red frame.
878
879 **<u>Figure S4</u>. Growth curves of WT and Δ*arcZ D. solani* strains used in this study.**
880 (A) Growth curves of D s0432-1, IPO 2222, their respective Δ*arcZ* mutants and IFB0223. The
881 latter (in grey) has a slight growth delay (Mann-Whitney test, p-value<0.05). (B) Growth curves
882 of strains used in complementation and heterologous expression tests. The plasmids do not
883 cause any growth defect in D s0432-1, IPO 2222 and Δ*arcZ* mutants. IFB0223 strains (in grey)
884 have growth delay already observed in the experiment without the plasmid (Mann-Whitney
885 test, p-value<0.05). All experiments were carried in 4 biological replicates.
886

887 **Figure S5. Alignment of *arcZ* sequences.** The *arcZ* DNA sequences were retrieved by
888 running a BlastN on the NCBI database using the *arcZ* sequence of *D. solani* D s0432-1 as
889 query. Search was limited to the *Dickeya* genomes. Then, the *Dickeya arcZ* sequences were
890 aligned with *E. coli* MG1655 *arcZ* by using Jalview [53] and Muscle [54]. Known regions of
891 interactions with the *pecT*, *flhD* and *rpoS* 5'UTR mRNA in *D. dadantii* and *E. coli* are indicated
892
893 **Supplementary Material and Methods.** DOCX file with supplementary material and
894 methods.
895
896 **Table S1. Distribution of the clusters *ssm*, *ooc*, and *zms* in 155 *Dickeya* strains whose**
897 **genome is sequenced.** For each *Dickeya* species, the strains were classified on the basis of
898 the presence or absence of the cluster *ssm*, *ooc*, and *zms*.
899
900 **Table S2. Lists of SNPs in *D. solani* IFB0099, D S0432.1, IFB0223, IPO3337 and IPO 2222.**
901
902 **Table S3. Strains and plasmids used in the study.**
903
904 **Table S4. Oligonucleotides used in the study.**

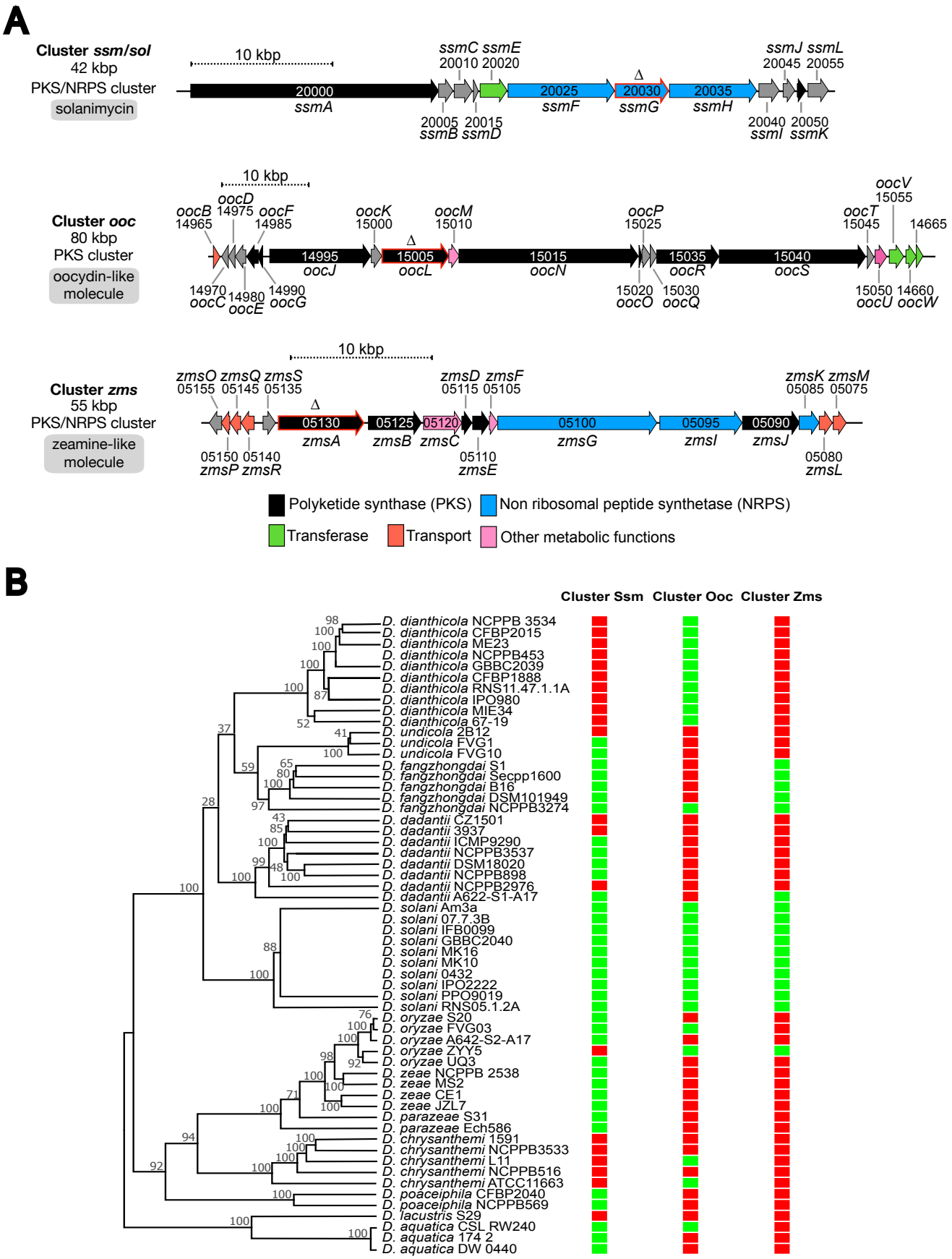

Figure 1: Organization and distribution of the secondary metabolite clusters *ssm*, *ooc* and *zms* of *D. solani* D s0432-1.

(A) Organization of the clusters *ssm, ooc,* and *zms.* Genes are indicated using the NCBI nomenclature of the NCBI reference genome sequence NZ_CP017453.1 of *D. solani* D s0432-1. XXXXX are the digital number in BJD21_RSXXXXX, which corresponds to the locus tag. Arrowheads show gene orientations. Color code indicates gene function. The red-framed arrows indicate genes targeted for in-frame deletion performed in this study. (B) MLSA tree positioning strains within the *Dickeya* genus. The evolutionary history was inferred by using the Maximum Likelihood method. The presence (green frame) or absence (red frame) of the cluster *ssm, ooc,* and *zms* are indicated in front of each strain. The distribution of these clusters in 155 *Dickeya* strains whose genome has been sequenced is given in Table S1.

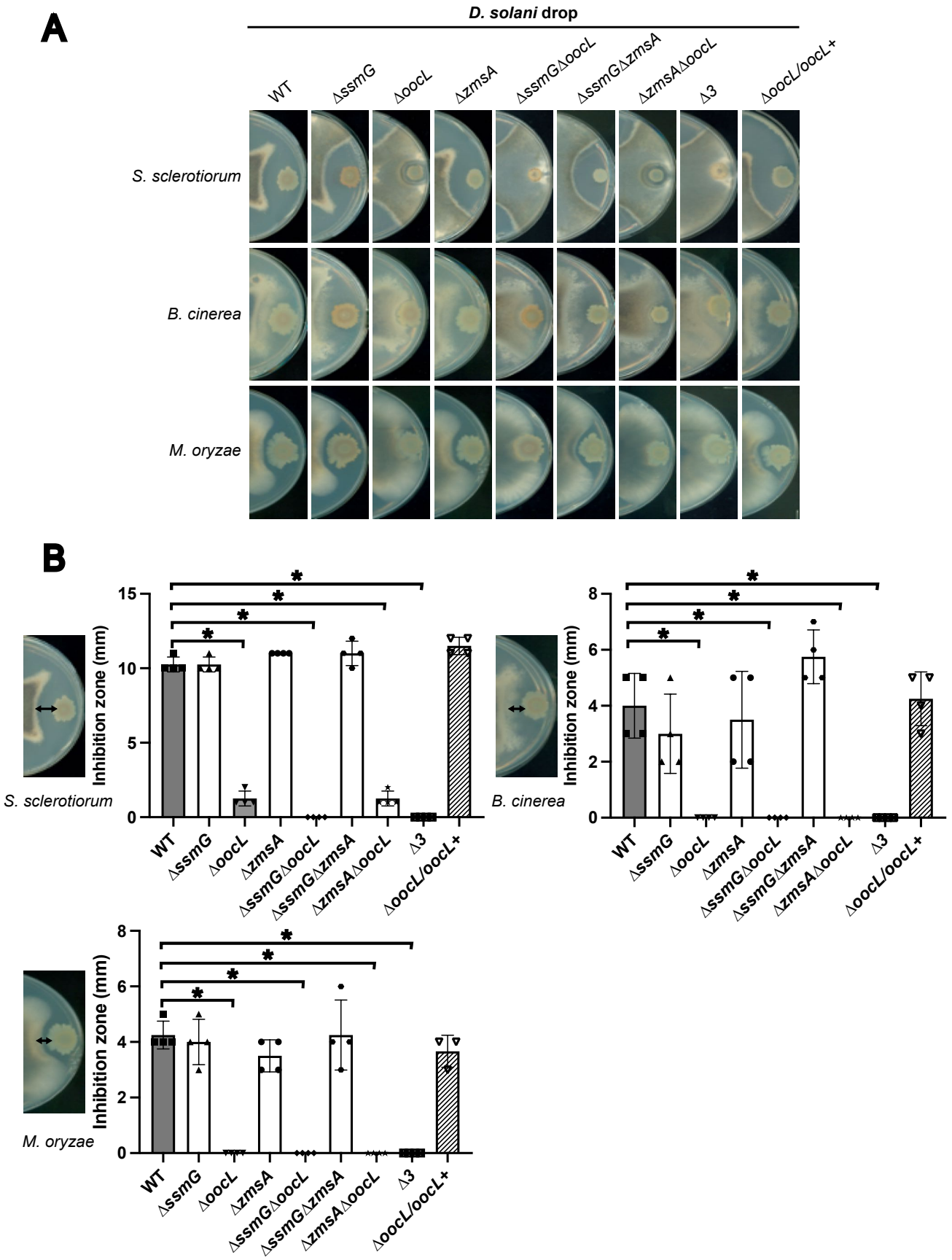

Figure 2: Inhibition of fungal growth by *D. solani* D s0432-1 and mutant derivatives.
5 µL of bacteria culture at OD_{600nm} = 2 from *D. solani* D s0432-1 (WT) or derivatives were spotted onto PDA plates inoculated with plugs of *S. sclerotiorum*, *B. cinerea* or *M. oryzae* mycelium. Plates were incubated at 25°C until the mycelium covers the plate. Lengths of fungi inhibition zone were measured in 4 independent experiments. A statistical difference was significant only between the WT and *ΔoocL* mutants (Mann-Whitney test; * p-value < 0.05).

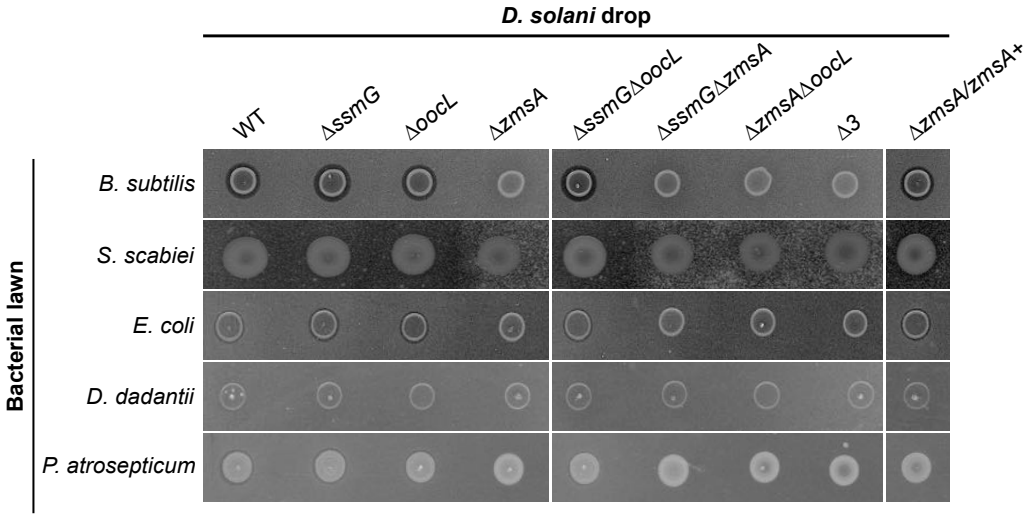

Figure 3: Inhibition of bacteria by *D. solani* D s0432-1 and mutant derivatives.
Bioassay plates were prepared by mixing bacterial culture (*B. subtilis, S. scabiei, E. coli, D. dadantii* and *P. atrosepticum*) with warm LB agar. 5 µL of bacterial cultures at OD_{600nm} = 2 from *D. solani* D s0432-1 (WT) or derivatives were spotted onto the plate and incubated at 30°C during 48h. A slight inhibition zone was observed with *B. subtilis* and *E. coli* plates, except with the *Δzms* mutants. All experiments were carried in 4 replicates.

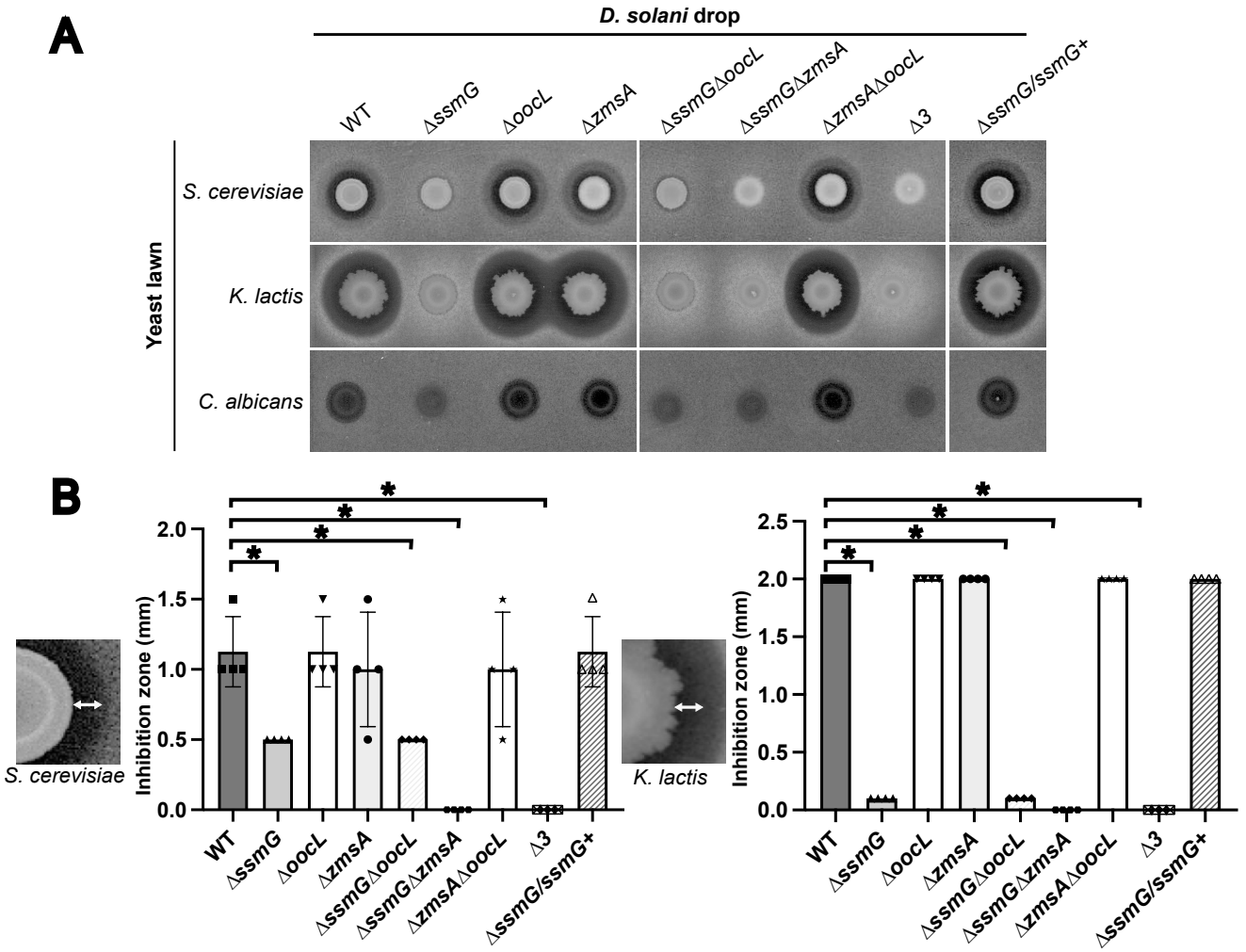

Figure 4: Inhibition of yeasts by *D. solani* and mutant derivatives.
Bioassay plates were prepared by mixing yeast culture (*S. cerevisiae, K. lactis, C. albicans*) with warm YPD agar. (A) 5 µL of bacterial cultures at OD_{600nm} = 2 from *D. solani* D s0432-1 (WT) or derivatives were spotted onto the plates and incubation was performed at 30°C during 48 h. (B) The radius of each inhibition zone was measured. A statistical difference was significant only between the WT and the *Δssm* mutants (Mann-Whitney test; * p-value < 0.05). For *C. albicans*, the inhibition zone was too small to be quantified. All experiments were carried in 4 replicates.

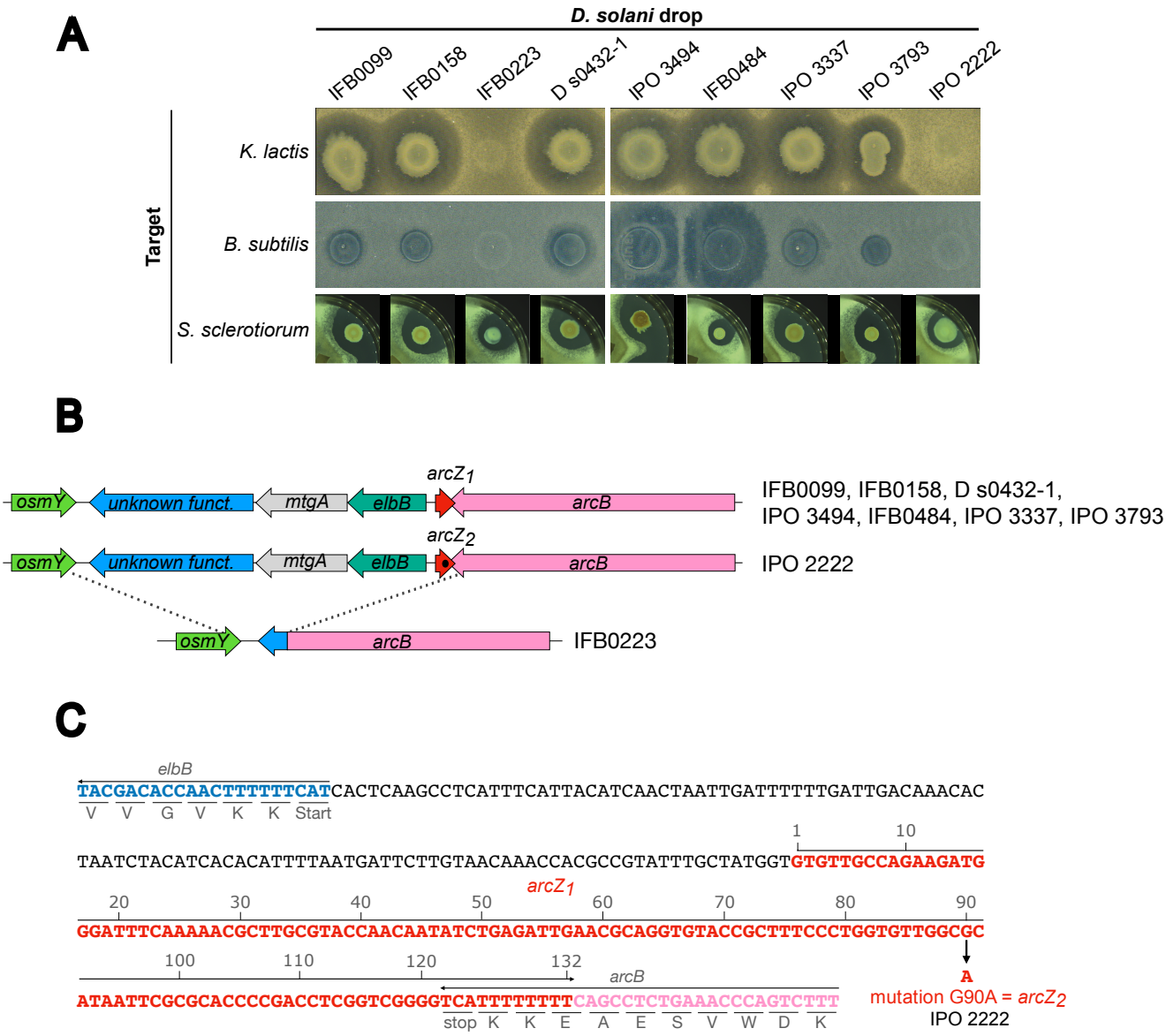

Figure 5: *D. solani* WT strains deficient for anti-microbial activity are mutated for the sRNA *arcZ*.

(A) Inhibition of *B. subtilis, K. lactis* and *S. sclerotiorum* by diverse WT *D. solani* strains. The tests were performed as previously described using the nine strains IFB0099 (NZ_CP024711), IFB 0158 (NZ_PENA00000000), IFB0223 (NZ_CP024710), D s0432-1 (NZ_CP017453), IPO 3494 (NZ_CM001842), IFB0484 (NZ_CM001860), IPO 3337 (NZ_CP016928), IPO 3793 (NZ_CP017454) or the type strain IPO 2222 (NZ_CP015137). Only IFB0223 and IPO 2222 were unable to inhibit *B. subtilis* and *K. lactis.* (B) Organization and conservation of the *arcZ* locus in the nine *D. solani* strains. The single mutation G90A in IPO 2222 *arcZ* is symbolized by a dark spot in the red *arcZ* arrow. (C) Zoom on the nucleotide sequence around *arcZ* of *D. solani* D s0432-1. This allele is named $arcZ_1$. Positions and orientations of the genes *elbB, arcZ* and *arcB* are indicated. The location of the G90A mutation present in IPO 2222 is indicated. This allele is named $arcZ_2$.

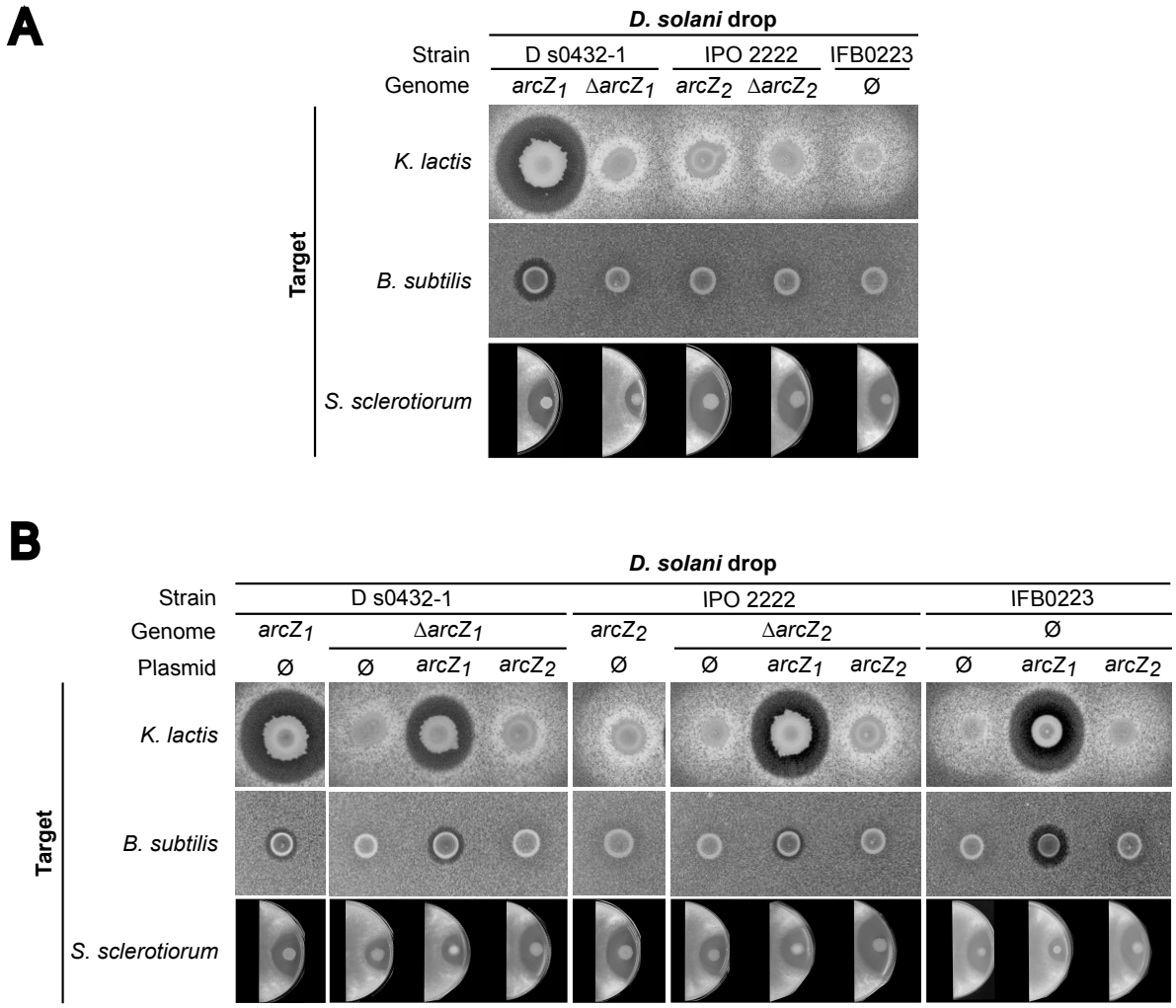

Figure 6: Inhibition of *K. lactis* and *B. subtilis* by *D. solani* is regulated by ArcZ.
Yeast bioassay plates were prepared by mixing culture of *K. lactis* with warm YPD agar. Bacteria bioassay plates were prepared by mixing culture of *B. subtilis* with warm LB agar. PDA plates were inoculated with plugs of *S. sclerotiorum*. For each experiment, 5 µL of bacteria culture at OD_{600nm} = 2 from the different *D. solani* strains were spotted onto the plate. (A) Inhibition zones observed with D s0432-1, IPO 2222, their respective Δ*arcZ* mutants and IFBO223. $ArcZ_1$ is required for the synthesis of metabolites produced by the clusters *ssm* and *zms* clusters (inhibition of *K. lactis* and *B. subtilis*, respectively) but not for the metabolite produced by the cluster *ooc* (inhibition of *S. sclerotiorum*).
(B) Complementation tests and heterologous expression of the alleles $arcZ_1$ or $arcZ_2$ in the three *D. solani* strains. $ArcZ_1$ activates the anti-microbial activities of *ssm* and *zms* clusters in IPO 2222 and IFBO223. All experiments were carried in 4 replicates.

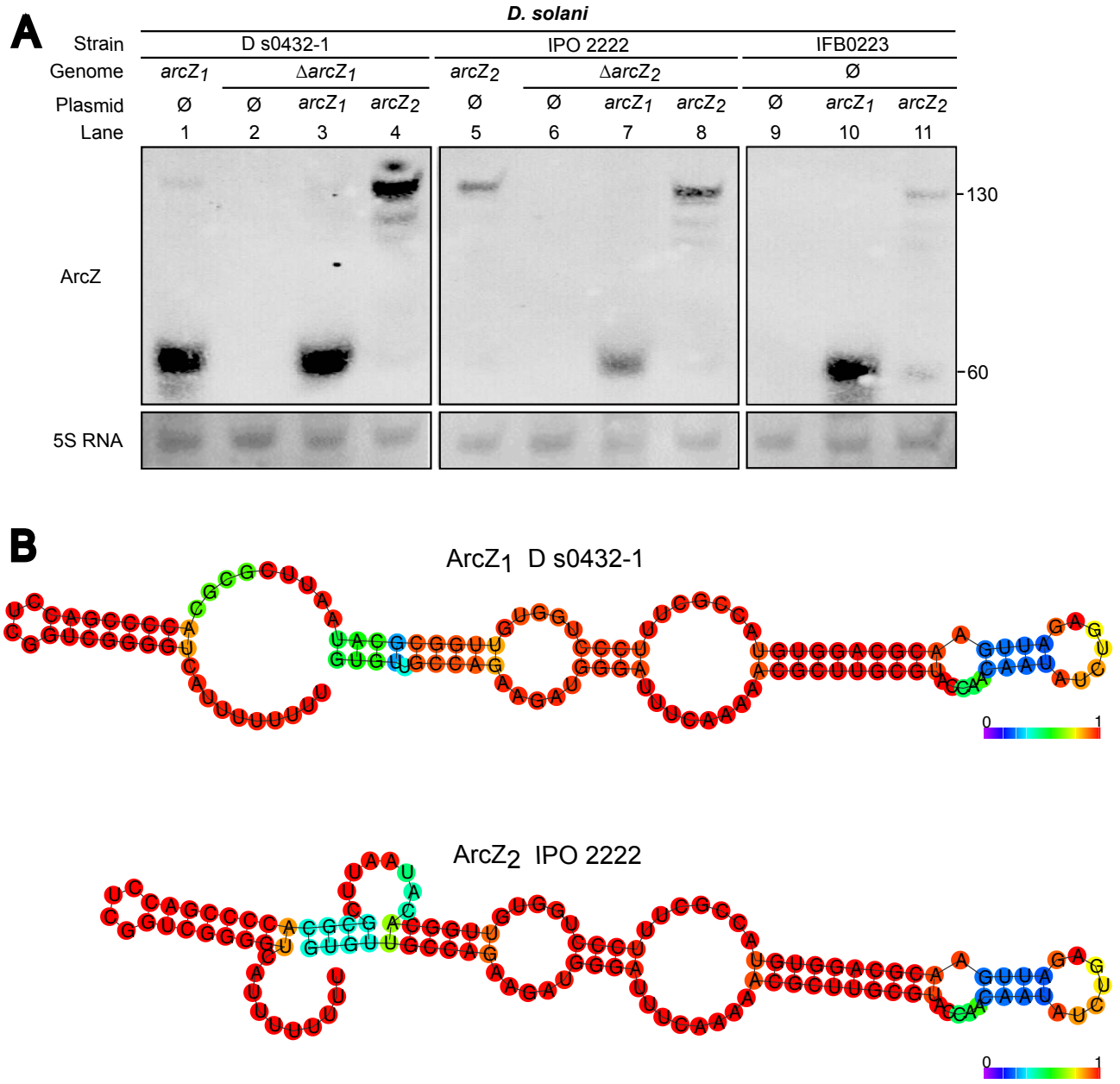

Figure 7. Expression of different ArcZ alleles: the G90A mutation in ArcZ$_2$ does not prevent its production but its processing.

(A) Detection of the sRNA ArcZ$_1$ and ArcZ$_2$ by Northern Blot in *D. solani* strains. A small transcript (~60 nt) corresponding to the processed 3′ fragment of ArcZ$_1$ was detected in D s0432-1 and in all strains expressing the allele *arcZ*$_1$ on plasmid. In IPO 2222, only the full-length form (~132nt) ArcZ$_2$ was detected, as well as in strains expressing the allele *arcZ*$_2$ on plasmid. The 5S RNA is used as a loading control. This experiment was performed twice with biological replicates and gave identical results. (B) Prediction of secondary of the precursor forms of ArcZ$_1$ and ArcZ$_2$ by RNA fold. Bases are colored according to base-pairing probabilities (see color scale). The G90A mutation present in ArcZ$_2$ seems to modify the structure of the ArcZ sRNA precursor.

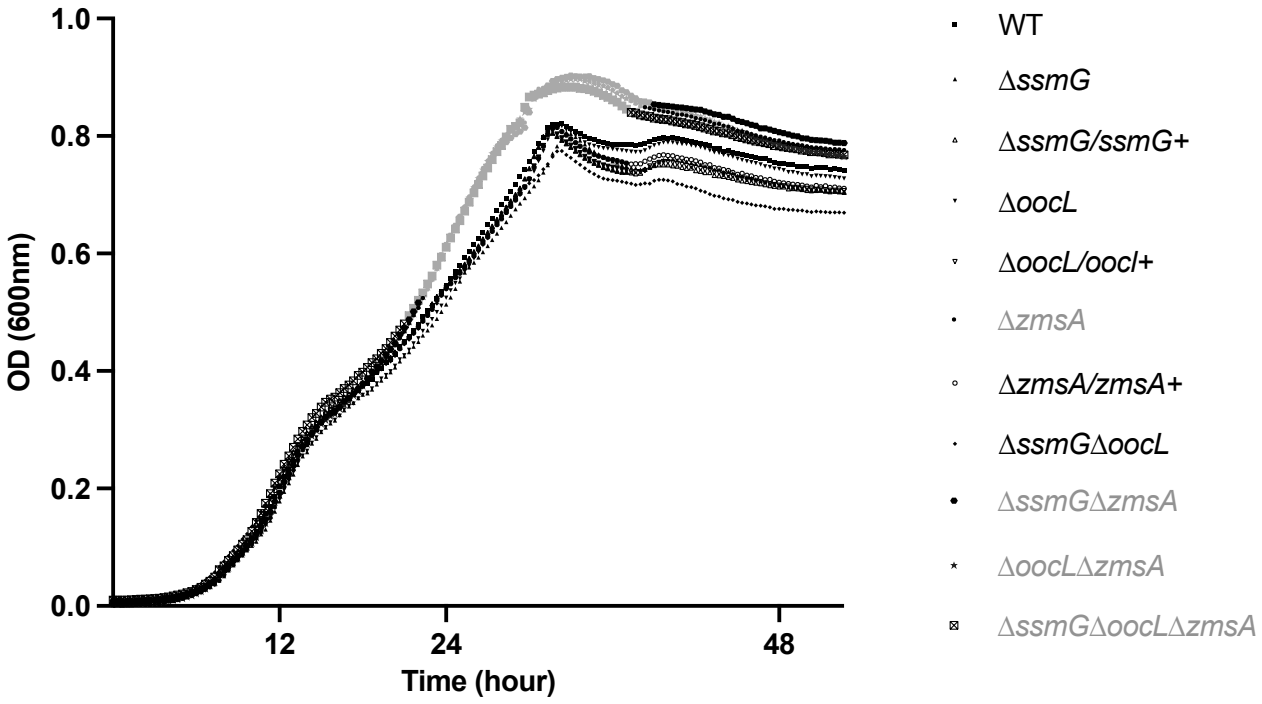

Figure S1. Growth curves of *D. solani* strains and mutant derivatives.
A 96-well plate containing M63 medium with 1% sucrose was inoculated with the strains used in this study at an OD of 0.06. The growth of each strain was determined by measuring OD_{600} every 20 minutes during 2 days in TECAN. The different strains showed similar overall growth, except for the light grey points where a low but significant fitness gain was observed for the mutants Δ*zms,* Δ*ssm* Δ*zms,* Δ*ooc* Δ*zms and* Δ*ssm* Δ*ooc* Δ*zms* (Mann-Whitney test, p-value<0.05).

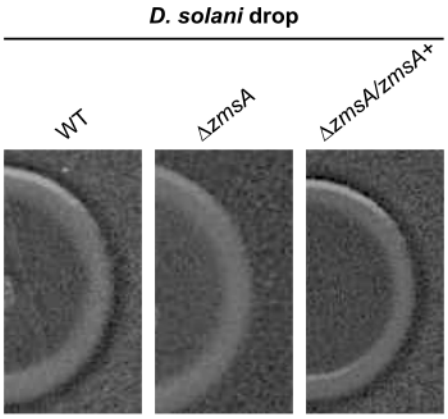

Figure S2. Inhibition of *E. coli* growth by *D. solani* D s0432-1 and mutant derivatives (zoom on drop borders).

Bioassay plates were prepared by mixing *E. coli* culture with melted LB agar as described in experimental procedures. 5 µL of bacterial culture at OD_{600nm} = 2 of *D. solani* D s0432-1 (WT) or derivatives were spotted onto the plate and incubated at 30°C during 48 h. A slight inhibition zone was observed except with the Δ*zms* mutant. All experiments were carried in 4 replicates.

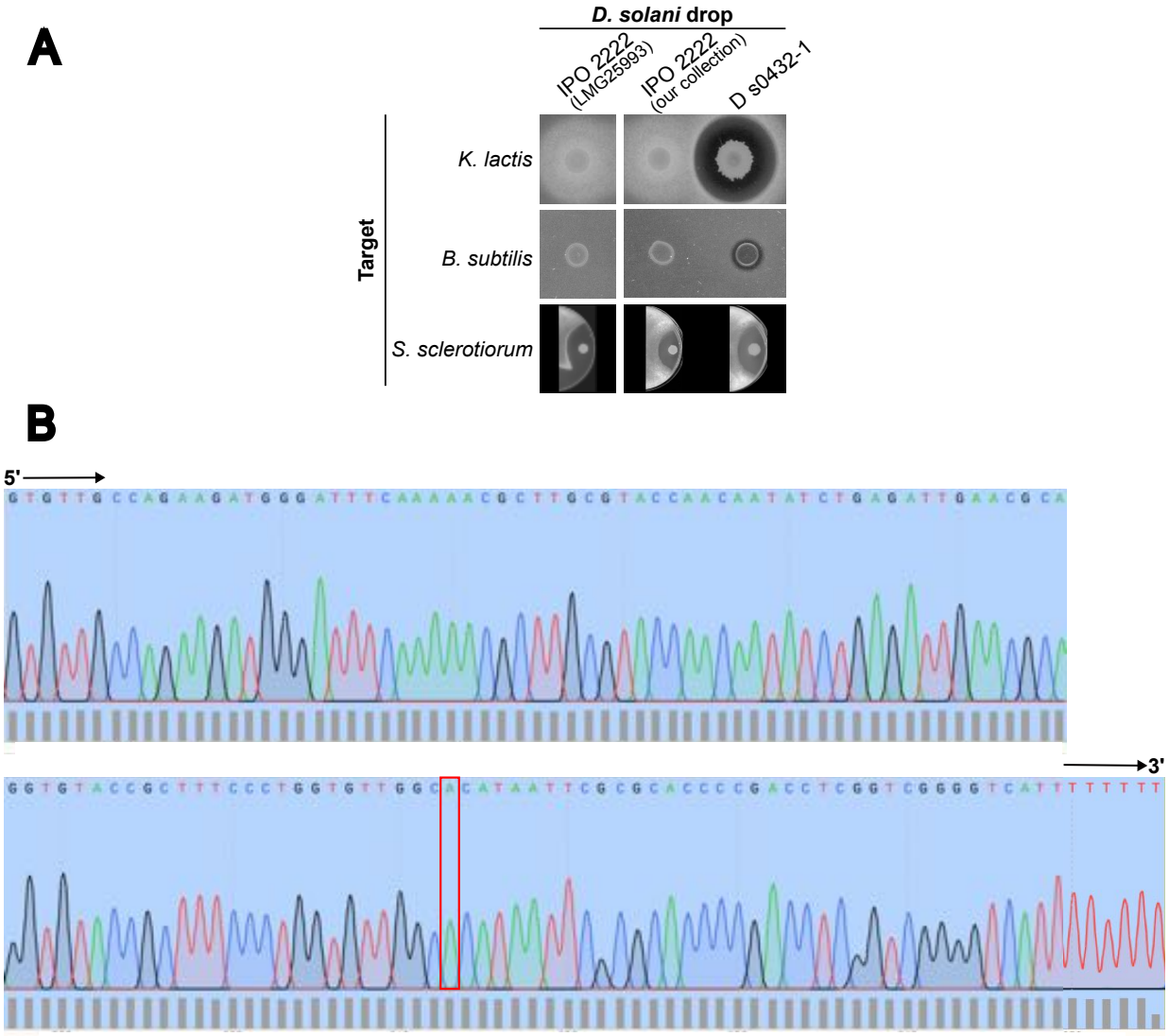

Figure S3. Phenotypes and *arcZ* sequence of WT *D. solani* IPO 2222 from the BCCM collection (LMG25993).

(A) Inhibition assay of *K. lactis*, *B. subtilis* and *S. sclerotiorum* by WT *D. solani* IPO 2222 LMG25993 from BCCM collection, compared to the strains used in this study.

(B) Sanger sequencing results of *D. solani* IPO 2222 *arcZ* (LMG25993)**.** The mutation G90A is highlighted by a red frame.

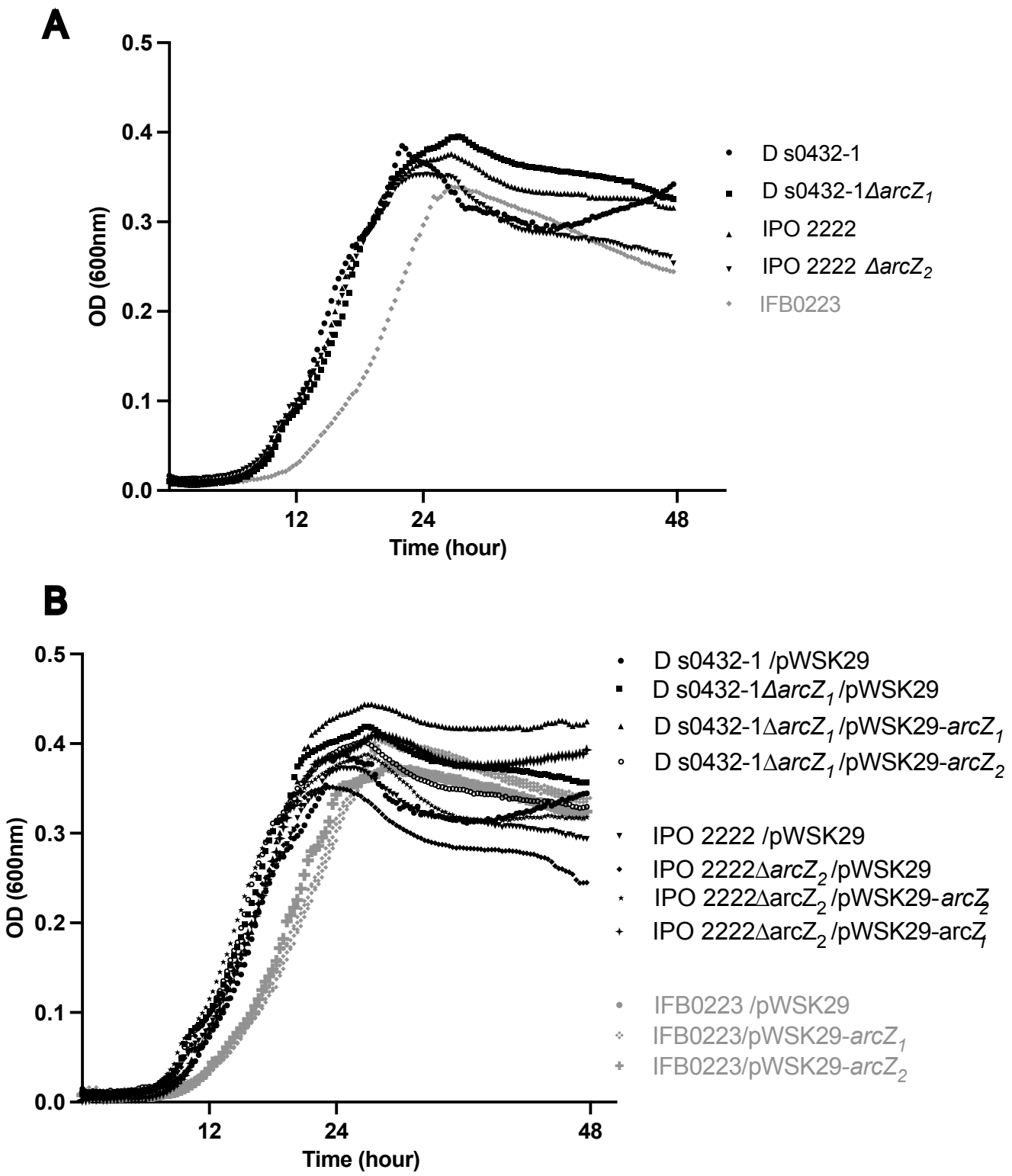

Figure S4. Growth curves of WT and Δ*arcZ D. solani* strains used in this study.
(A) Growth curves of D s0432-1, IPO 2222, their respective Δ*arcZ* mutants and IFB0223. The latter (in grey) has a slight growth delay (Mann-Whitney test, p-value<0.05). (B) Growth curves of strains used in complementation and heterologous expression tests. The plasmids do not cause any growth defect in D s0432-1, IPO 2222 and Δ*arcZ* mutants. IFB0223 strains (in grey) have growth delay already observed in the experiment without the plasmid (Mann-Whitney test, p-value<0.05). All experiments were carried in 4 biological replicates.

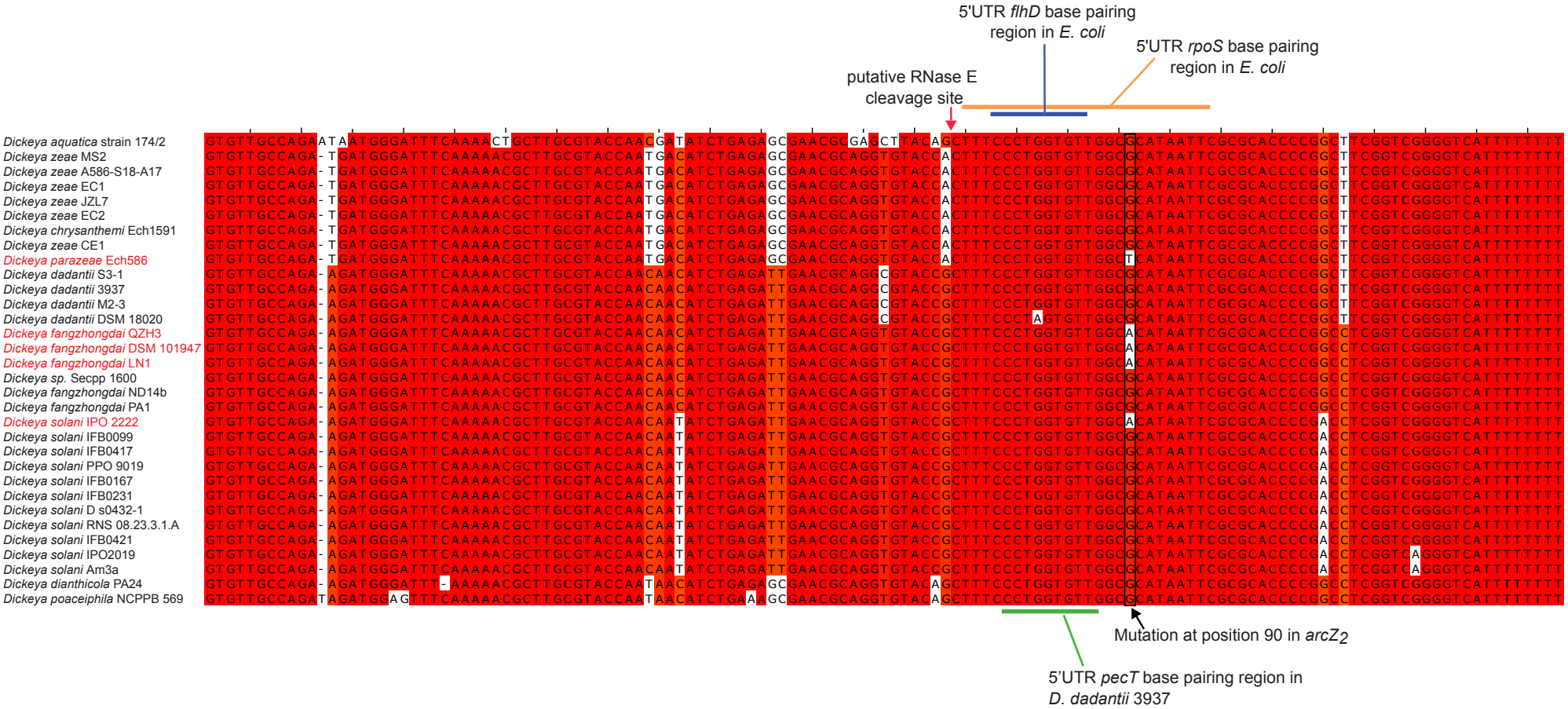

Figure S5. Alignment of *arcZ* sequences.

The *arcZ* DNA sequences were retrieved by running a BlastN on the NCBI database using the *arcZ* sequence of *D. solani* D s0432-1 as query. Search was limited to the *Dickeya* genomes. Then, the *Dickeya arcZ* sequences were aligned with *E. coli* MG1655 arcZ by using Jalview (56) and Muscle (57). Known regions of interactions with the *pecT*, *flhD* and *rpoS* 5'UTR mRNA in *D. dadantii* and *E. coli* are indicated